NEW CONSTRUCTIONS OF GLULAM BEAMS IN CANADA

by

NAHULESALINGAM MOHADEVAN

B.Sc.Eng., The University of Peradeniya, 2000
M.Phil., The University of Preadeniya, 2003

A THESIS SUBMITTED IN PARTIAL FULFILLMENT OF
THE REQUIREMENTS FOR THE DEGREE OF

MASTER OF APPLIED SCIENCE

in

THE FACULTY OF GRADUATE STUDIES

(Forestry)

THE UNIVERSITY OF BRITISH COLUMBIA

July 2007

ABSTRACT

An optimized 24f glulam beam lay-up has been investigated with a series of laboratory testing and computer modeling. The basic ideas of these assessments are to increase the efficient use of timber resource in the glulam construction with integration of reliability based procedures to characterize the specified strengths for the glulam beams.

During this study, existing grade specifications in the Canadian Standards have been refined. Five new Douglas fir lamina grades (T1, Cc, B, C and D) and their tensile strength data have been established.

Finite element glulam analysis program ULAG has been used for the primary beam modeling and analysis. New routines to account for the laminating effects on the beam strength and to evaluate the shear capacity of the glulam beams have been incorporated in the ULAG program. The shear stress output from the finite element analysis has been integrated to consider weakest link stress volume effect for the shear capacity assessment. Subsequently 24f glulam beams have been successfully simulated using the refined ULAG program. A similar analysis based on ASTM D3737 has been carried out using the US-GAP program based on a detailed knot survey on the new lamina grades.

The model has been calibrated by full scale test results. The model predictions and the corresponding assessments have been further validated by a second set of full scale glulam bending and shear tests. Glulam beams 305 mm and 610 mm deep, have been tested to assess the flexural strength. Three sets of glulam beams, 305 mm and 457 mm deep have been tested at short span to depth ratios to determine the shear capacity. Excellence prediction accuracy by ULAG has been confirmed.

Table of Contents

3. Development of New Lamina Grades

4. Lamina Strength Assessment

5. Glulam Beam Modeling

LIST OF TABLES

Page Number

LIST OF FIGURES

Page Number

Acknowledgements

I wish to express my sincere appreciation to my supervisor Prof. Frank Lam for his invaluable guidance and support during this research. His comments, suggestions and criticisms strengthened my confidence in formulating and finalizing this thesis. I also acknowledge him for the financial support provided to me during this period.

My sincere thanks to Prof. Ricardo Foschi, emeritus professor for his expertise assistance during the research especially for his guidance in the ULAG modeling. I also like to extent my thanks to Prof. David Barrett and Dr. Bryan Russell Folz for their support extended during the study.

The continuous assistances and coordination of Mr. Kent Fargey and Mr. Travis Van de Vliert throughout this research is greatly acknowledged. I am also grateful to Dr. Borjen Yeh for his technical assistance, feedback and support during the research.

I also would like to extent my sincere thanks to Mr. Bob Myronuk, Mr. George Lee, Mr. Larry Tong and other technical staff members attached to the Wood Mechanics Laboratory for their supports during the laboratory testing.

The assistances and funding from the industrial partners, especially Western Archrib-Structural Wood Systems and the Natural Resources Canada Value to Wood Program is greatly acknowledged.

Chapter 1

INTRODUCTION

1.1GENERAL BACKGROUND

Glue laminated timber (Glulam) is a type of engineered wood product that has improved performance and attributes compared to solid sawn members leading to very efficient use of the timber resource. In North America the minimum requirements for the manufacturing of Glued laminated timber (Glulam) beams are specified in CSA O122 M89 (Canada) and ANSI/AITC AI90.1 (US). CSA O122 M89 uses visual grading and modulus of elasticity (MOE) assessment to build different grades of glulam while ANSI additionally requires the knot distribution of the material to be considered. CAN/CSA 0122 M89 specifies four grades of lam-stock B-F, B, C and D. B-F is the highest grade designated for the extreme tension zones of 20f and 24f beams. For this grade, knots or other similar defects exceeding 10 mm and local slope of grain steeper than 1:16 shall not be permitted within 13 mm of the edge of the outer tension face lamination after finishing. D is the weakest grade, generally placed at the mid zone of the beam. The laminating boards of this grade are allowed to have knot sizes up to 50% of the board width.

The current Canadian specifications generally deal with pre-established lamina grades and specify whether the given beam lay-up is admissible. The US procedures require tedious knot assessments to qualify the material grade. It is recognized that there is a need for more efficient beam design procedures which will increase the performance of the glulam beams as well as improving the efficient use of timber resource.

One of the key-issue from the glulam manufacturers' point of view is the availability of supply of the high grade material needed for the extreme tension zone of the 24f beams. Here the interest is to investigate the possibility to modify some of the knot size restrictions at the extreme tension zone of the 24f beams in order to match the strength requirements to the knot size characteristics of the lamina resource for the tension lamina-grades.

In the past there were many studies targeting various aspects of glulam beam design and construction were reported. In Canada the glulam analysis computer model ULAG, Ultimate Load Analysis of the Glulam, was developed by Folz and Foschi (1992). In the United States GAP, Glulam Analysis Program, developed based on ASTM D3737 is recognized as the tool to configure new lay-up and construction of glulam beams.

ULAG is a stochastic finite element program developed at the University of British Columbia. The program can simulate virtual construction of glulam beams/columns and progressive loading until collapse to investigate the bending capacities and failure behaviors of the glulam. Therefore, the program has high potential to be use in exploring the structural performance of glulam with new lay-ups and/or new lamina grades.

At this point the idea of the current research is to develop new lamina grades to construct more efficient 24f glulam lay-ups as well as verify/fine-tune ULAG predictions. The information will subsequently be used to develop reliability based specified strengths for implementation in Canadian Codes.

1.2 AIMS AND OBJECTIVES

The current research focused on three main aims as given below :

- Develop new Douglas-fir laminae lay-ups for the construction of glulam beams.
- Verify/fine-tune/upgrade/validate ULAG performances.
- Analyze the strength characteristics and failure behavior of full scale-24f glulam beams.

These developments will enhance the glulam design and analysis and facilitate the Glulam-Industry/researcher to achieve the following objectives in the long run,

- Expand the use of glued-laminated beams (glulam) by establishing reliability-based procedures to qualify/optimize new construction (grades/species/lay-up) of glulam in the Canadian Codes.
- Develop the associated test data for predicting the performance (bending strength and stiffness) of high performance glulam beams in engineering applications.

1.3 RESEARCH PLAN

The research plan has three phases namely : Development (Phase I), Assessment (Phase II) and Verification (Phase III). Phase I deals with the initial literature survey, grade development process, and assessment of the lamina strength properties required for the beam modeling. Phase II focused on the glulam beam modeling/analysis using ULAG and GAP to assess the performance of new grades and the calibration of the ULAG model. This analysis will facilitate the design of target 24f glulam beams for the verification tests as well. The final verification tests and the subsequent assessments were carried out during Phase III. A detailed flow of the research plan is given in Figure 1.1.

Figure 1.1 Research plan

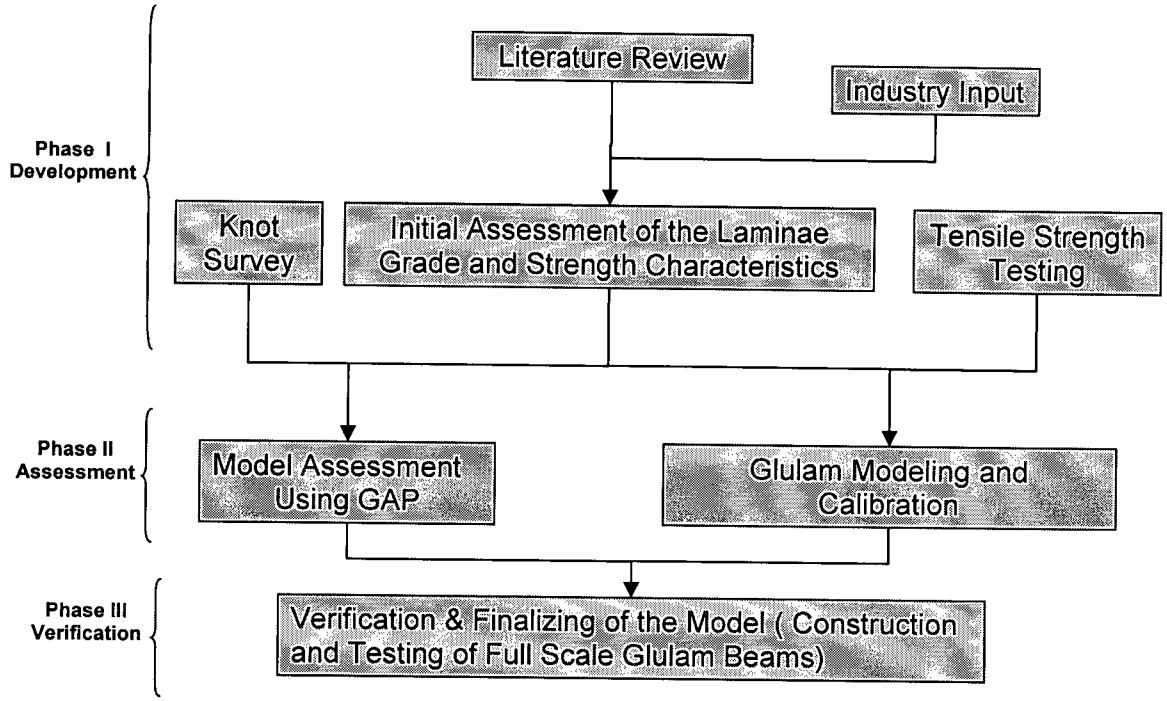

1.4 SCOPE OF THE TESTING

The current research requires a series of laboratory testing. The scopes of these tests are given below.

(I) Grade Development and Knot Survey (38 mm x 140 mm lamina)

4.88 m long lamina ~ 500 boards

2.44 m long lamina ~ 200 boards

These assessments were focused on developing a database for five new lamina grades.

(II) Tension Testing (38 mm x 140 mm lamina)

Four tension lamina grades T1, B, C and D were considered for the tension testing. These tests were carried out in three groups corresponding to 4.88 m and 2.44 m long laminae and finger joints.

4.88 m long lamina - four grades @ 100 boards/grade

2.44 m long lamina - four grades @ 100 boards/grade

Finger joint - four grades @ 100 boards/grade

(III) Full Scale Beam Testing

Glulam bending tests : 3rd point loading test.

Two sets of tests were carried out; 0.30 m deep beams were tested during ULAG calibration process and 0.61 m deep beams were tested during the verification phase. Each of these sets consisted of twenty four beams.

0.30 m deep 24f glulam beams tested at 21 span to depth ratio

0.61 m deep 24f glulam beams tested at 18 span to depth ratio

Glulam shear tests: four point loading test.

Three sets of beams were tested during the glulam shear assessments; two sets of 0.30 m deep beams were tested during the ULAG calibration process and one 0.46 m deep beam was tested during the verification phase. Each of these sets consist twenty four beams.

0.30 m deep 24f glulam beams tested at 6 span to depth ratio

0.30 m deep 24f glulam beams tested at 7 span to depth ratio

0.46 m deep 24f glulam beams tested at 6 span to depth ratio

1.5 ORGANIZATION OF THE THESIS

Chapter one of this thesis provides general background of the study and discusses the key aims and objectives of the research. This chapter also provides details of the scope of the laboratory testing, the research plan and the organization of the thesis.

Chapter two describes the glulam beam strength characteristics and the computer models. It details the general lamina strength characteristics, glulam design parameters and discusses on the glulam beam modeling.

Chapter three focuses on the grade development for the new lamina grades. This chapter describes the step by step assessments procedures carried out during the grade development process.

Chapter four details the lamina strength assessment procedures. This chapter mainly presents the tensile strength test results of the laminae and finger joints. An illustration of the Maximum Likelihood Evaluation (MLE) procedures used for finger joint strength assessments and the details of knot survey are also discussed in this chapter.

Chapter five provides the information about the ULAG upgrading and the details of the subsequent ULAG analyses of full scale glulam bending and shear calibration tests. The details of the GAP assessments are given at the latter part of this chapter. This chapter also describes the glulam shear volume effect analysis and the reliability based normalization procedures carried out to obtain specified strengths of the glulam beams.

Chapter six gives the details of the glulam verification tests. The information about the full scale glulam bending and shear tests is described at the initial part of this chapter. Size effect assessment and reliability analysis corresponding to 0.30 m and 0.61 m deep glulam beams tested are given in the latter part of this chapter.

Chapter seven presents the summary of the research carried out, key outcomes, concluding remarks and the recommendations for the future study.

1.5.1 UNIT USED

The beam dimensions were originally measured in imperial unit as practiced in the industry. However for computation/numerical analysis purposes the SI units were adopted during the analysis/assessments. Therefore the SI units have been used as the primary unit throughout this dissertation and in some instances beam dimensions were given in both imperial and SI unit systems for convenience.

Chapter 2

Glulam : State of the Art

2.1 INTRODUCTION

In North America, glulam beams are produced with lay-up and laminae specifications based on the Canadian standard -CAN/CSA-O122-M89 and American standard ASTM D3737. These standards provide guidelines for the assessment/qualification of the lamina grades and the beam lay-ups. In Canada, 20f E and 24f E are commonly manufactured glulam grades. Generally these beams were constructed to yield a modulus of elasticity (MOE) of 12,400 MPa (1.8 million psi).

In addition there are many glulam beam analysis models available to evaluate different beam lay-ups and lamina properties. One of the initial works was the computer model GLULAM developed by Foschi and Barrett (1980). Glulam Analysis Program (GAP) is another glulam design tool developed based on ASTM D 3737. Folz and Foschi (1997) developed a computer model ULAG to predict the capacity and failure behavior of the glulam beams. This model is considered to be one of the most versatile tools to analyze the glulam beam failure behavior.

Douglas fir, southern pine and hem fir are the main species used in North American glulam construction. Initially the lumber is sawn into a standard 38 mm thick lamina and graded. The graded boards are then end joined using finger joint and gluing techniques according to standard specifications. One of the major advantages of using finger joined boards is that the length of the beam will not be limited by the length of the lamina boards. In this way, the finger jointing is a vital part of the glulam beam.

Furthermore, the glulam technique makes it possible to use material from small trees to construct very large beams. However, this finger jointing process can reduce the net strength of the laminae and thereby may control the overall strength of the glulam beam.

2.2 GLULAM MODELS

2.2.1 GLULAM

Foschi and Barrett (1980) developed a finite element model-GLULAM to predict the statistics of the strength of glulam beam. This model uses the MOE, tensile strength, compression strength and the knot distribution to simulate a number of gulam beams. The model basically considers 154 mm wide lamina boards. Based on model simulation, each element will be assigned a net strength σ_c and a modulus of elasticity Ec. Then the finite element model can be used to perform beam loading/failure simulations. The beam failure is determined by the brittle fracture of the weakest element. The model was originally calibrated and verified using a trial and error fit based on tensile strength test results. The model was not calibrated to assess the influence of finger joints.

2.2.2 GAP

This is an analytical program based on ASTM D 3737. The program mainly utilizes the data from full scale laminae tests, knot distribution, and slope of grain information corresponding to the laminating grades to predict the beam strength.

The allowable properties for a structural glued laminated timber lay-up is specified as the products of stress index values, stress modification factors and adjustment factors for end use condition (ASTM D3737). Here the stress index values are

species dependent and established based on laboratory testing. The bending stress index values for the visually graded and E-rated lumber are given in ASTM D 3737. The adjustment factors for the end use condition are given in the Section 9 of the above standard. The stress modification factors are determined based on the knot distribution and the corresponding MOE values.

2.2.3 ULAG

ULAG (Ultimate Load Analysis of Glulam) is a one dimensional linear stochastic finite element program. The main advantages of this program are that it has the capacity to simulate a virtual construction of glulam beams and analyze the progressive loading until collapse. This program can be used to investigate the beams bending and shear strength capacities and critical failure behaviors. It doesn't require any knot data as input.

The key strength parameters required for the assessment are the tensile strength test data of the lamina and finger joint and the corresponding MOE values. These data were inputted to the program as text data files and processed using an auxiliary program ULAGDAT1 which generates the primary data file ULAGDAT1.dat with the summary statistics of the strength data corresponding to the material grades considered. The lamina length details of the material grades used for the beam construction were stored in a secondary data file ULAGDAT2.dat using another auxiliary program ULAGDAT2.

Based on these data the ULAG program simulates the virtual construction of glulam beams. The key processes followed during the beam simulation are given below.

1. Randomly pick the laminating boards from the lamina stock of various length groups representing the actual material supply for the beam production.
2. Place the boards in sequence at corresponding beam layers to form the beam and determine the finger joint locations.
3. Formulate the finite element mesh and determine the nodal locations.
4. Assign random- MOE values to each piece of lamina in the beam corresponding to the material grade considered.
5. Provide beam's support and loading conditions.
6. Assign the stochastic flexural strength to each segment of the lamina between the nodes corresponding to the material grade considered.
7. Derive a finite element solution for the problem.
8. Assess the axial deformations along the beam axis.
9. Evaluate the non linear normal and shear strain distribution at each of the nodal sections across the beam.
10. Determine axial stresses.
11. During beam loading simulation identify the preliminary lamina failure within the beam based on the exceeding of the axial stress over the lamina strength assessed at each of the lamina segments between the nodes.
12. Replace the stiffness and strength of the failed lamina segment with null values and repeat steps 7 to 12 until collapse of the beam.
13. Record the failure load, deflection failure type and other details of interest.
14. Repeat the steps 1 to 13 until getting the required sample size to obtain the statistics of the beam capacities and failure data.

2.3 GLULAM FLEXURAL STRENGTH

Tensile strengths of lamina and finger joints and the MOE of the laminating boards are the key factors to determine the strength/capacity of the beam. These factors are species dependent and controlled by the grade of the lamina. Generally the capacity of the beams is given in terms of the specified strength. The typical glulam specified strength ranges from 25 MPa to 35 MPa. This is about 20% higher than the flexural capacity of the corresponding solid sawn timber beams.

Timusk (1997) reported results of two sets of 30 spruce-pine-fir (SPF) glulam beam tests and four sets of SPF C and B grade lamina and finger joint tension tests. These testing were carried out as part of the ULAG calibration/verification program. The beams, 0.30 m and 0.46 m in depth, were built with 38 mm nominal thickness lamination. They were tested with a four point loading setup at a 16 span to depth ratio. The 0.30 m beams had eight C grade laminae and the 0.46 m deep beam had two B grade tension lamination and ten C grade lamination. Average MOR values of these two sets are 35.5 MPa and 38.3 MPa, respectively. A high correlation between the tensile strength of the extreme lamina and the flexural strength of the beam was observed. Different patterns of failure were reported for the beam tests. However, initial failure behavior was not identified due to the sudden collapsing nature of the failures.

2.4 GLULAM SHEAR STRENGTH

Yeh and Williamson (2001) studied the shear strength of full size glulam beams using four point test method. The beams had a span of 3.05 m with a span to depth ratio of approximately 6.7. The test consists of five sets of beams, two for Douglas fir, two for

southern pine and one for SPF. The Maximum Likelihood Evaluation procedure was used to analyze the censored data. An overall 70% of shear failures with mean shear strength values of 4.5 MPa, 5.5 MPa and 4.5 MPa were reported for Douglas fir, southern pine and SPF, respectively. The resultant coefficients of variation (COV) values are 7.5%, 9% and 12%, respectively. The corresponding characteristics strength values are about 30% lower than the ASTM small block shear test results. Although, this is a significant reduction, the results demonstrated that significantly higher (35%-60%) allowable shear strength can be justified.

2.4.1 SHEAR STRENGTH MODELS

Foschi and Barrett (1976) developed a technique to determine the longitudinal shear strength of wood beams based on the Weibull's theory of brittle fracture. The method relates the survival probability of the two wood volumes under different loading conditions and predicts the critical loads for one volume based on the failure load of the other one. A sequence to predict the longitudinal shear strength based on the ASTM block shear test was established.

Lam et al. (1997) investigated the shear strength of Canadian soft wood structural lumber based on a series of laboratory tests and numerical modeling. A two span five point test procedure with span to depth ratios of 6 and 5 were used for the laboratory assessments and a finite element assessment incorporating the Weibull weakest link theory was used for the numerical predictions. A very good model performance with a maximum 6% error was demonstrated.

2.5 TENSILE STRENGTH OF LAMINA

Timusk (1997) reported tensile strength values of 38 mm x 140 mm spruce-pine-fir C and B grade laminae and finger joints. Average tensile strengths of C and B grade laminae tested at 3.66 m gauge length, are 24.0 MPa and 33.0 MPa, respectively. Corresponding COV are 25% and 18%. Average tensile strength values of the finger joined C and B grade boards are 26.5 MPa (COV = 23%) and 33.7 MPa (COV = 20%), respectively. The finger joined boards had a gauge length of 1.22 m and only boards failed at the finger joints were used for the assessment.

Marx and Evans (1988) reported the tensile strength of laminating grades of 38 mm x 140 mm Douglas-fir and southern pine lumber. The highest Douglas fir grade L1 had an average tensile strength value of 34.3 MPa and the corresponding southern pine No. 1D grade had 34.5 MPa. The overall coefficient of variation and the mean modulus of elasticity for these grades are 30% and 14,800 MPa, respectively.

2.5.1 LAMINATING EFFECTS

Falk and Colling (1994) investigated the laminating effects in the European and North American glulam beams. Influence of three key factors: 1) effect of test procedures, 2) reinforcement of defects, and 3) dispersion of low-strength lumber on the bending strength was discussed. Overall laminating factor ranges of 1.06 to 1.59 for European glulam and 0.95 to 2.51 for North American glulam were reported.

2.6 LAMINATING GRADES

CAN/CSA -0122-M89 specifies four laminating grades B-F, B, C and D for the construction of glulam beams. B-F is the highest grade designated for the extreme tension zones of 20f and 24f beams. Here the 20f and 24f beams have allowable bending strength of 13.8 MPa and 16.5 MPa, respectively. For this grade, knots or other similar defects exceeding 10 mm and local slope of grain steeper than 1:16 shall not be permitted within 13 mm of the edge of the outer tension face lamination after finishing. D is the weakest grade, generally placed at the mid zone of the beam. The laminating boards of this grade are allowed to have knot sizes up to 50% of the board width.

2.7 KNOT SURVEY

ASTM D 3737 provides guidelines to establish the knot frequency distribution in the laminating grades. This data will be used to establish the beam lay-ups and the allowable properties for the structural glue laminated timber. A sample consisting of a minimum of 100 pieces or 300 m of lumber randomly chosen from a representative group is required to assess each of the grades considered.

A set of nine types of knots and their measurement procedures are outlined in ASTM D 3737. All the knots greater than 6 mm of equivalent cylindrical cross-section need to be measured.

Finally the statistical parameters of the knot data can be used to guide the building of new glulam beams with new lay-ups.

Chapter 3

Development of New Lamina Grades

3.1 INTRODUCTION

The initial guidelines for the new lamina grades were proposed by Mr. Kent Fargey (Western Archrib - Structural Wood Systems). This consists of the specifications for a set of seven laminating grades T1, T2, Cc, B, C, Dc, and D. Here T1 and T2 are tension lamina grades and Cc and Dc are compression lamina grades. Each of these grades is intended to match different levels of stresses developed across the glulam beam. In beam applications under positive moment, generally, the lamina grades corresponding to the bottom layers will be subjected to the maximum tensile stress, the top layers are expected to bear high compressive stresses, and the middle layers will be subjected to a lower level of axial stresses.

Douglas fir 38 mm x 140 mm laminae were used for all the grade assessment and verifications. Lamina samples were randomly selected from the mills and delivered to UBC as batches. The first four batches of material were used for the primary grade development process and verification. These batches consist of one hundred and eighty nine 2.44 m long boards and five hundred and nine 4.88 m long boards.

The development process consists of a series of grading analysis and testing. Grading was conducted by the combination of E rating and visual grading as specified in the new guidelines. Initially the grade yield and the grade distribution across the samples were analyzed. Then the guidelines were modified to improve the grade yield. After confirming that sufficient grade outturn for the potential lamina grades, the samples were

tested in tension to assess the strength distribution. In October 2005, a results review was carried out by experts from the industry and UBC. This visit was focused on fine-tuning the guidelines to improve the grade properties. Subsequently an additional edge distortion restriction was proposed for the T1 grade material to improve the lower tail of the strength distribution. The finalized grade set was inspected and verified by Mr. Allan Rosek, Executive Director, National Lumber Grades Authorities (NLGA).

3.2 DEVELOPMENT PROCEDURE

Initially three batches of material were graded according to the proposed specifications aiming to identify the resource distribution; therefore, some of the very minor grading criteria were not followed. The key grading factors considered for the resource assessment are given in Table 3.1 and the resource distribution obtained is given in Tables 3.2 and 3.3.

Table 3.1 Key grading factors considered for the resource assessment-Trial I

(Assessment date: July 7, 2004, Material: 38 mm x 140 mm Douglas fir laminae)

Parameter	T1	T2	B	C_c	C	Dc	D
$MOE_{(min)}$, GPa	13.1	13.1	13.1	13.1	11.0	11.0	-
$MOE_{(average)}$, GPa	15.4	15.4	15.4	15.4	12.0	12.0	-
Knot size, mm	35	35	35	55	55	70	70
Edge knot, mm	23	35	-	-	-	-	-
Slope of grain (all 4 sides)	1:16	1:16	1:16	1:12	1:12	1:08	1:08
Pith (maximum allowed) [1]	1/8 of cross section						
Clear wood, %	67	60					
Spacing between strength reducing characteristics (SRC), mm	600	600					
Knot spacing near finger joint [2]	2Φ	2Φ					

Notes:

1. Pieces containing wide growth rings or lightweight pith associated wood at the end of the piece occupying over $1/8^{th}$ of the cross-section shall be excluded.
2. Any knot over 10 mm in diameter shall not occur within 2 knot diameters (Φ) of any finger joint.

Table 3.2 MOE values of the first three batches of material

MOE range, GPa		Number of boards			Total length, m
Less than	Greater than or equal to	Batch 1	Batch 2	Batch 3	
-	15.2	55	3	4	168
15.2	14.5	15	9	11	134
14.5	13.8	11	6	10	105
13.8	13.1	21	14	13	183
13.1	12.4	19	20	26	271
12.4	11.7	20	32	23	317
11.7	11.0	14	32	25	312
11.0	-	34	73	48	673
Total		189	189	160	2,163

Table 3.3 Grade outturn corresponding to Trial I

MOE range, GPa		Grade		Number of boards		Total length, m	Grade yield, m						
Less than	Greater than or equal to		Batch 1	Batch 2	Batch 3		T1	T2	B	Cc	C	Dc	D
11.0	-	D	34	72	48	668							668
11.7	11.0	C	13	32	25	310					310		
		Dc	1	0	0	2						2	
		D	0	0	0	0							0
12.4	11.7	C	20	32	23	317					317		
		Dc				0						0	
		D				0							0
13.1	12.4	C	18	20	26	268					268		
		Dc	1	0	0	2						2	
		D				0							0
13.8	13.1	T1	8	0	4	39	39						
		T2	1	4	4	41		41					
		B	5	0	1	17			17				
		Cc	7	10	4	85				85			
		Dc				0						0	
		D				0							0
14.5	13.8	T1	7	2	1	32	32						
		T2	1	1	1	12		12					
		B	1	2	2	22			22				
		Cc	2	2	6	44				44			
		Dc				0						0	
		D				0							0
15.2	14.5	T1	10	7	4	78	78						
		T2	1	1	2	17		17					
		B	1	0	2	12			12				
		Cc	3	1	3	27				27			
		Dc				0						0	
		D				0							0
-	15.2	T1	39	1	3	115	115						
		T2	0	0	0	0		0					
		B	8	0	0	20			20				
		Cc	6	2	1	29				29			
		Dc				0						0	
		D	1	0	0	2							2
		R*	1										
Total Length, m			**189**	**189**	**160**	**2158**	**263**	**71**	**71**	**185**	**895**	**5**	**675**

R - rejected board which did not confirmed with the specifications.*

The grade outturn from trial-I shows a fairly low yield for the T2, B and Dc grades. With subsequent discussions between industry experts and UBC team, it was decided to drop Grade Dc from the grade set.

Based on this outcome, the initial grade proposal was modified to further mobilize the material resource across the grades considered. Mainly the MOE values of B grades and Cc grades were lowered to 12.4 GPa in order to re-distribute some high quality boards from the C grade group to the B and Cc grade groups. Some of the key grading factors of the modified guidelines are given in Table 3.4 and the corresponding grade outturn is given in Table 3.5.

Table 3.4 Key grading factors considered for the resource assessment-Trial II
(Assessment date: March 1st 2005, Material : 38 mm x 140 mm Douglas fir laminae)

Parameter	T1	T2	B	C_c	C	D
$MOE_{(min)}$, GPa	13.1	13.1	12.4	12.4	11.0	-
$MOE_{(average)}$, GPa	15.4	15.4			12.0	-
Knot size[1], mm	35	35	35	55	55	70
Edge knot, mm	23	35	-	-	-	-
Slope of grain (all 4 sides)	1:16	1:16	1:16	1:12	1:12	1:08
Pith (maximum allowed)[2]	1/8 of cross section					
Clear wood, %	67	60				
SRC spacing, mm	600	600				
Knot spacing near finger joint[3]	2Φ	2Φ				

Notes:

1. For T1 and T2 all knots within 200 mm length is summed. For all other grades, including B, C and D, knots are summed according to the criteria set out in clauses 4.2.1.7 and 4.2.1.8 of the modified grading specifications as given below:

Clause 4.2.1.7 Knots shall be measured between lines enclosing the knot and parallel to the edges of the wide faces. If two or more knots are in line, ie, partially or completely enclosed by the same parallel lines and separated lengthwise by less than 200 mm, the effective width of the knots shall be the distance between two parallel lines which enclose the knots.

Clause 4.2.1.8 When two or more knots appear in the same cross section of a piece (Opposite each other on a face or edge), the sum of their sizes shall not exceed the maximum permitted knot size.

2. Pieces containing wide growth rings or lightweight pith associated wood at the end of the piece occupying over $1/8^{th}$ of the cross-section shall be excluded.
3. Any knot over 10 mm in diameter shall not occur within 2 knot diameters (Φ) of any finger joint.

Table 3.5 Grade outturn corresponding to Trial II

MOE range, GPa		Grade	Number of boards				Total length, m	Grade yield, m						
Less than	Greater than or equal		Batch 1	Batch 2	Batch 3	Batch 4		T1	T2	B	Cc	C	D	R
11.0	-	D	33	72	46	81	1051						1051	
		R				0	0							
12.4	11.0	C	30	63	48	42	819					819		
		D	1	1	0	0	7						7	
		R	3	0	1	0	12							12
13.1	12.4	B	12	18	21	16	297			297				
		Cc	0	0	0	0	0				0			
		C	3	2	6	3	61					61		
		D	1	0	0	0	2						2	
		R	1	0	0	0	2							2
13.8	13.1	T1	10	7	6	6	117	117						
		T2	1	0	1	0	7		7					
		B	3	0	3	0	22			22				
		Cc	6	7	3	0	63				63			
		C	0	0	0	0	0					0		
		D	1	0	0	0	2						2	
		R	1	0	0	1	7							7
-	13.8	T1	52	16	10	10	302	302						
		T2	3	0	1	0	12		12					
		B	6	1	9	0	63			63				
		C	2	0	0	0	5					5		
		Cc	7	2	5	1	56				56			
		D	2	0	0	0	5						5	
		R	11	0	0	0	27							27
Total length, m			**189**	**189**	**160**	**160**	**2943**	**419**	**20**	**383**	**119**	**885**	**1068**	**49**

The laminae graded with the above guidelines were inspected and verified by Mr. Allan Rosek (Executive Director, NLGA)

Again the resource distribution was assessed and very low yield for grade T2 observed. At this point tensile strength tests on the new grades were carried out to assess the strength characteristics of the new grades. It was observed that some of the weakest T1 grade boards which failed with lower load (~ 25 MPa) were caused by a combination of edge knot and local slope of grain deviation. Therefore, following changes were further proposed to improve the strength values at the lower tail of the distribution.

1. **Clear wood** (board with no edge distortion, no edge defect such as knot, knot hole, local slope of grain deviation etc.): Each lamina shall have at least 2/3 (67%) clear wood free of strength reducing characteristics with a slope of grain no steeper than 1:16.

2. **Clear Wood** (boards with edge distortion) : Any cross section (200 mm) which has any edge defect (knot, knot hole, local slope of grain deviation, etc.) shall have at least 75% clear wood free of strength-reducing characteristics with a slope of grain no steeper than 1:16.

The typical change in the strength distribution due to the changes in the grade specifications are illustrated in Figure 3.1. It is clear that changes to the grade have minimal impact on the overall tensile strength distribution eventhough some of the lower strength pieces are eliminated by the new grading rules.

Figure 3.1 Tensile strength distribution of T1 grade (Batch 5)

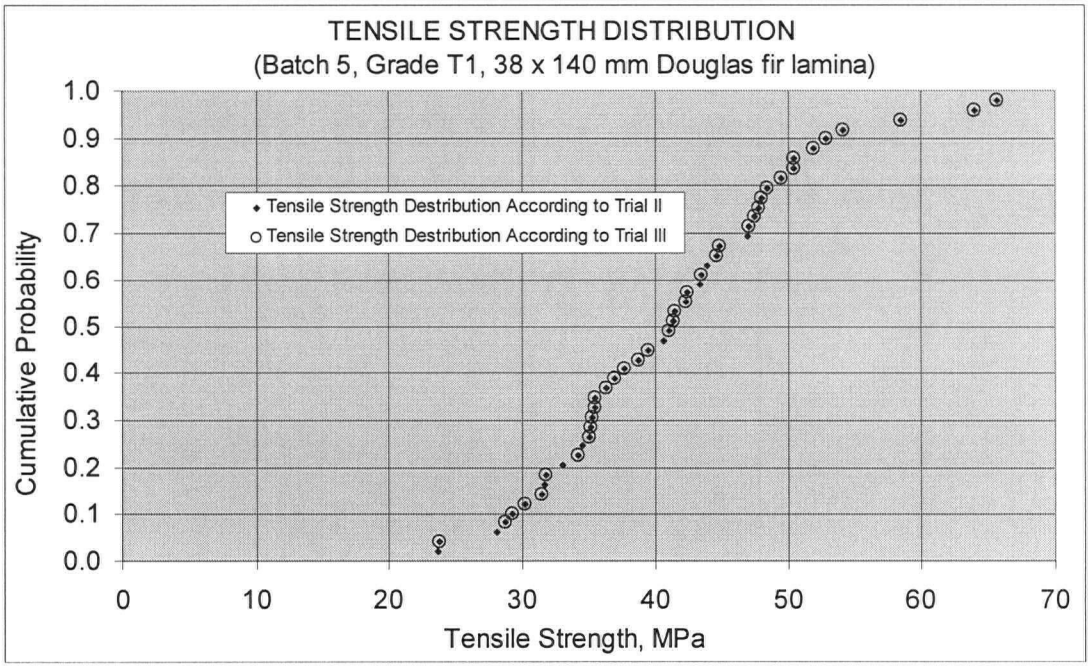

During the subsequent re-grading and assessments following observations were made:

1. The bending T1 grade has acceptable strength distribution.
2. The material resource has been fairly distributed between the grades T1, Cc, B, C and D.
3. The grade T2 has a very small (a total of 20 m length) yield.

Based on these outcomes the grade T2 was dropped from the grade set.

The finalized grade set consists of five potential grades : T1, Cc, B, C and D. The details of the final grade yield for these grades are given in Table 3.6.

Table 3.6 Grade outturn corresponding to Trial III

Grade	Number of boards					Total length, m
	Batch 1	Batch 2	Batch 3	Batch 4	Total	
T1	62	23	16	16	117	419
B	25	19	35	16	95	403
Cc	13	9	8	1	31	119
C	35	65	54	45	199	885
D	38	73	46	81	238	1,068
Rejected (R)	16	0	1	1	18	49
Total	189	189	160	160	698	2,943

Chapter 4

Lamina Strength Assessment

4.1 INTRODUCTION

The strength of laminae plays a major role in determining the load carrying capacity of glulam beams. Here the strengths of interest are the tensile strength and MOE of the laminae which are considered to be critical in common beam loading conditions. The magnitudes of these parameters are mainly controlled by the lamina grade specifications. Therefore, it is a necessity to determine these parameters each time when the grade specifications changes. The MOE of the boards can be determined using non-destructive test methods. Destructive tensile strength test is the only accurate means to measure the lamina tensile strength.

Tensile strength tests were carried out in this study to determine the strengths of the laminae and the finger joints. As mentioned in Chapter 2, strength of the laminating boards, strength of the finger joints and the distribution of the finger joints determine the overall strength of the laminae. The distribution of the finger joints is controlled by the length of the glulam beam and the length distribution of the laminae used for its construction. These factors have been taken in to account during the beam modeling process.

Shear capacity is another important parameter considered in the glulam beam design. Here the main concern is the shear strength of the D grade material which is generally placed at the middle shear core of the beam. ASTM small clear block shear test and the short span beam bending tests are the two standard test methods available to

assess the shear strength of the core material. On the other hand, it is recognized that the capacity of a beam in shear is influenced by its stressed volume. Therefore, ASTM small clear shear block tests are considered to be not appropriate to determine generalized shear strength of the laminae (Foschi and Barrett 1976, Lam et al. 1997). Therefore, the use of a numerical model is needed to assess the shear capacity of the glulam beam. Verification/fine-tuning of the model can be performed using full scale shear beam testing. The details of these assessments are discussed in Chapters 5 and 6.

Compressive strength of the laminae is another important factor in glulam beam design. However, this is not considered to be critical within the scope of the current study and is ignored in the modelling and analysis.

ASTM D3737 specifies the glulam design procedures based on the knot distribution of the laminating boards to determine the allowable properties of the structural glued laminated timber. As part of the study a detailed knot survey was carried out to assess the performance of the new lamina grades based on ASTM D3737.

4.2 MODULUS OF ELASTICITY

The MOE of the boards was measured during the grade development process using the Metriguard Model 340 E-Computer system. Summary statistics of the MOE test results are given in Table 4.1.

Table 4.1 Summary statistics of the MOE test results

Grade	T1	Cc	B	C	D
Mean, MPa	15,226	14,155	13,683	11,774	9,992
Standard deviation (SD), MPa	1,753	941	1,224	664	1,684
COV, %	12	7	9	6	17
Total number of boards tested	184	44	223	201	138

4.3 TENSILE STRENGTH TESTS I - LAMINA

Approximately 750 lamina specimens of the four tension laminating grades, T1, B, C and D were tested in tension parallel to grain. A Metriguard tension testing machine with full resistant grips and a capacity of about 450 kN was used for the testing. The tests were carried out at two gauge lengths 3.66 m and 1.22 m with a 0.61 m grip length at each end. For each grade the speed of loading was adjusted to maintain an average failure time of 10 minutes.

The mean tensile strength values corresponding to the T1 grade tested at 3.66 m and 1.22 m gauge length are 42.9 MPa and 52.6 MPa, respectively. Based on this values a length effect factor k of 5.4 was established for the material tested. The relationship between the strength values and the corresponding material volume (Lam 2000) used in the assessment of k factor is given in equation 4.1.

$$\frac{\tau_1}{\tau_2} = \left(\frac{V_2}{V_1}\right)^{\left(\frac{1}{k}\right)} \qquad (4.1)$$

In the equation 4.1 τ and V corresponds to the tensile strength and the volume of the material, respectively. The subscripts 1 and 2 refer to the samples corresponding to the two different volumes considered.

Then all the lamina strength values were size adjusted to a 2.44 m gauge length in order to establish a unique set of reference strength data. This database was used as input for the ULAG analysis. The summary statistics of the lamina tensile strength test are given in Table 4.2 and the corresponding tensile strength distributions are given in Figure 4.1.

Table 4.2 Summary statistics of the tensile strength test results at 2.44 m gauge length

Grade	T1	B	C	D
Mean, MPa	49.8	34.8	29.4	24.0
SD, MPa	12.2	8.0	9.4	6.5
COV, %	24	23	32	27
Total number of boards	184	223	201	138

Figure 4.1 Tensile strength distributions of the new lamina grades

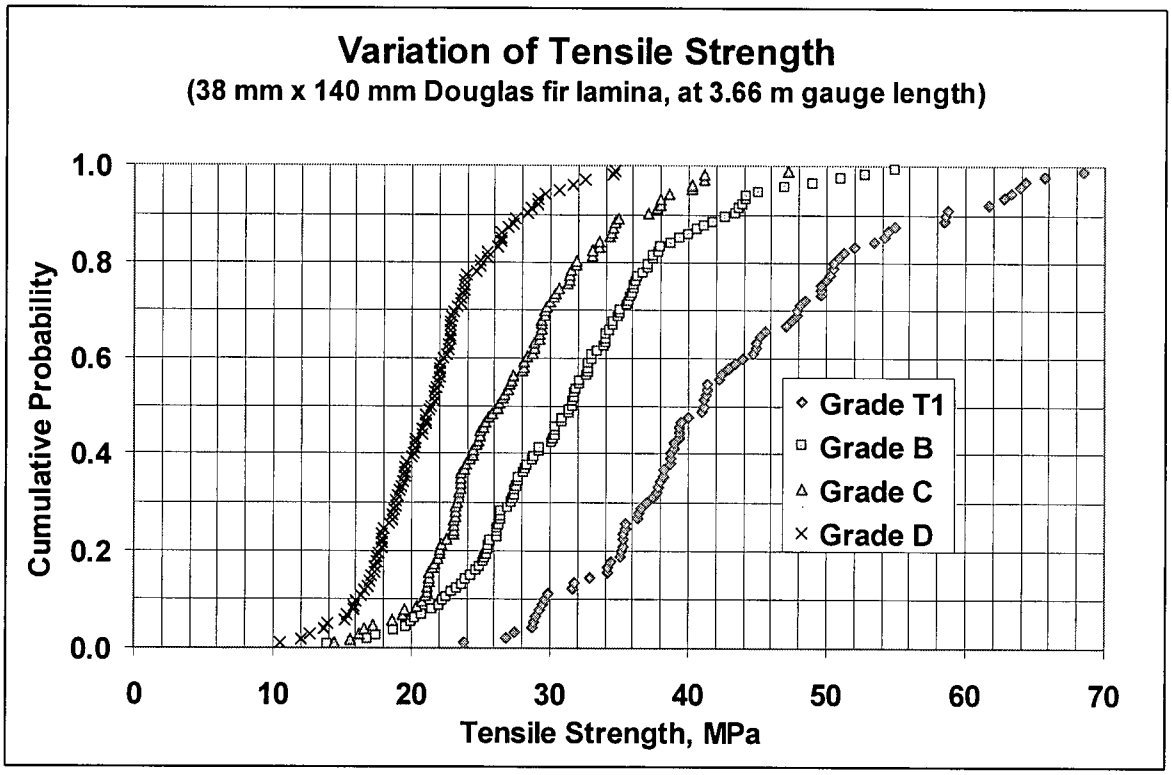

Images of some of the T1 grade material failed at low strength level is given in Figure 4.2

Figure 4.2 Images of some of the T1 grade material failed at low strength level

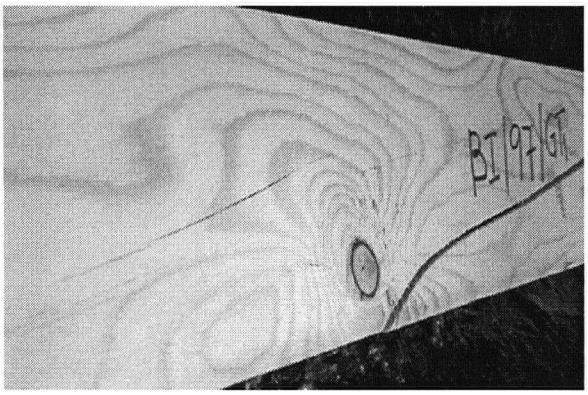

(a)

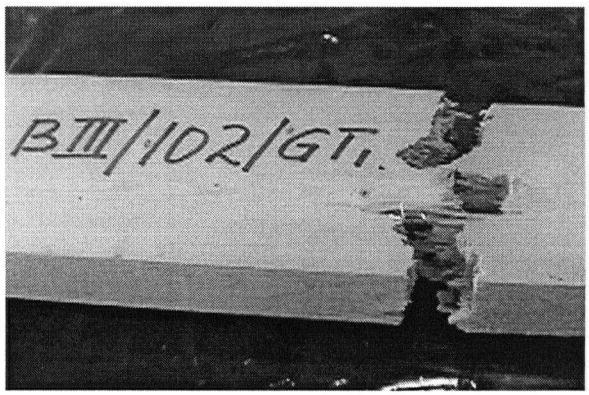

(b)

(c)

(d)

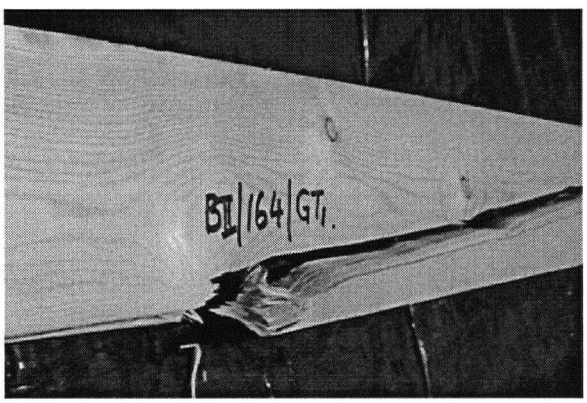

(e)

(f)

4.4 TENSILE STRENGTH TESTS II - FINGER JOINT

Approximately four hundred finger joined lamina specimens of the four grades, T1, B, C and D were tested in tension to determine the finger joint strength. Here the gauge length and the grip lengths were kept at 0.66 m and 1.22 m, respectively. Again the speed of loading was kept to achieve a time to failure of approximately 10 minutes.

As expected, both lamina and finger joint failures were observed during the tests. This resulted in two set of strength data: one corresponding to the finger joint failure cases and the other corresponding to the lamina failure cases where the finger joint strength is higher than that of the failure load of the specimen. This issue of mixed failure modes was sorted out using the Maximum Likelihood Evaluation (MLE) theory to isolate the strength of finger joints from a censored database. A computer program based on this theory was developed to carry out the assessments.

4.4.1 MLE ASSESSMENTS

As mentioned earlier the MLE assessments were performed to establish the un censored data for the finger joint strength. This procedure will be later used for the assessment of glulam beam shear capacity as well.

The theoretical formulation of this program is discussed below:

Consider two continuous random variables x, s and the corresponding statistical parameters θ.

x_i- primary data

s_i – suspended data

θ_i – statistical parameters.

Then the likelihood functions L_1 and L_2 corresponding to the primary and suspended data can be written as,

$$L_1(primary) = \prod_{i=1}^{n} f(x_i / \theta_i) \tag{4.2}$$

$$L_2(suspended) = \prod_{i=n+1}^{N} [(1 - F(s_i / \theta_i)] \tag{4.3}$$

where $f(x_i/\theta)$ and $F(s_i/\theta)$ are probability density function and cumulative distribution function, respectively.

Now for the likelihood of obtaining primary and secondary data, the total likelihood function can be written as,

$$L = L_1 L_2$$

For a 2p-Weibull distribution, the probability density function $f(x_i/\theta)$ and cumulative distribution function $F(s_i/\theta)$ can be written as fallows.

$$f(x_i / \theta) = \frac{k}{m}\left(\frac{x_i}{m}\right)^{k-1} e^{-\left(\frac{x_i}{m}\right)^k} \tag{4.4}$$

$$F(s_i / \theta) = 1 - e^{-\left(\frac{x_i}{m}\right)^k} \tag{4.5}$$

Then the logarithmic likelihood function can be written as,

$$\ln(L) = \sum_{i=1}^{n} \ln\left[\frac{k}{m}\left(\frac{x_i}{m}\right)^{k-1}\right] - \sum_{i=1}^{N}\left(\frac{x_i}{m}\right)^k \tag{4.6}$$

The maximum likelihood estimators of θ_i were obtained by maximizing ln(L).

The parameters m and k corresponding to the maximum value of equation 4.6 have been obtained by a trial and error-MLE program written in FORTRAN.

4.4.2 FINGER JOINT TEST RESULTS

The summary statistics of the finger joint test results are given in Tables 4.3 and 4.4. The distribution of the finger joint strength with a comparison of test specimen's strength is given in Figures 4.3 to 4.6.

Table 4.3 Details of the finger joint failures

Grade	T1	B	C	D
Total number of specimen tested	126	100	104	100
Number of finger joint failures	110	67	46	31

Table 4.4 Details of the finger joint strength values predicted by MLE program

Grade		T1	B	C	D
2P Weibull strength parameters	m, MPa	45.1	43.8	35.5	30.7
	k	5.4	5.6	6.1	5.3
Mean, MPa		41.59	40.48	32.96	28.28
COV, %		21	21	19	22

Figure 4.3 Tensile strength distribution of the T1 grade 38 mm x 140 mm Douglas fir finger joints

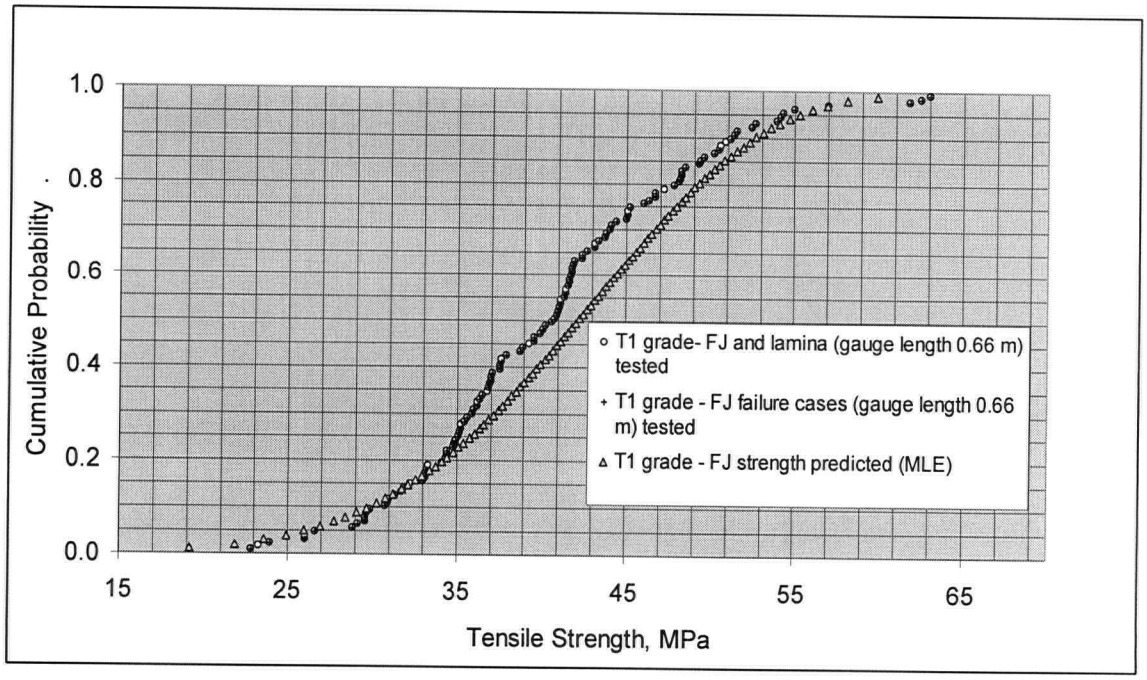

Figure 4.4 Tensile strength distribution of the B grade 38 mm x 140 mm Douglas fir finger joints

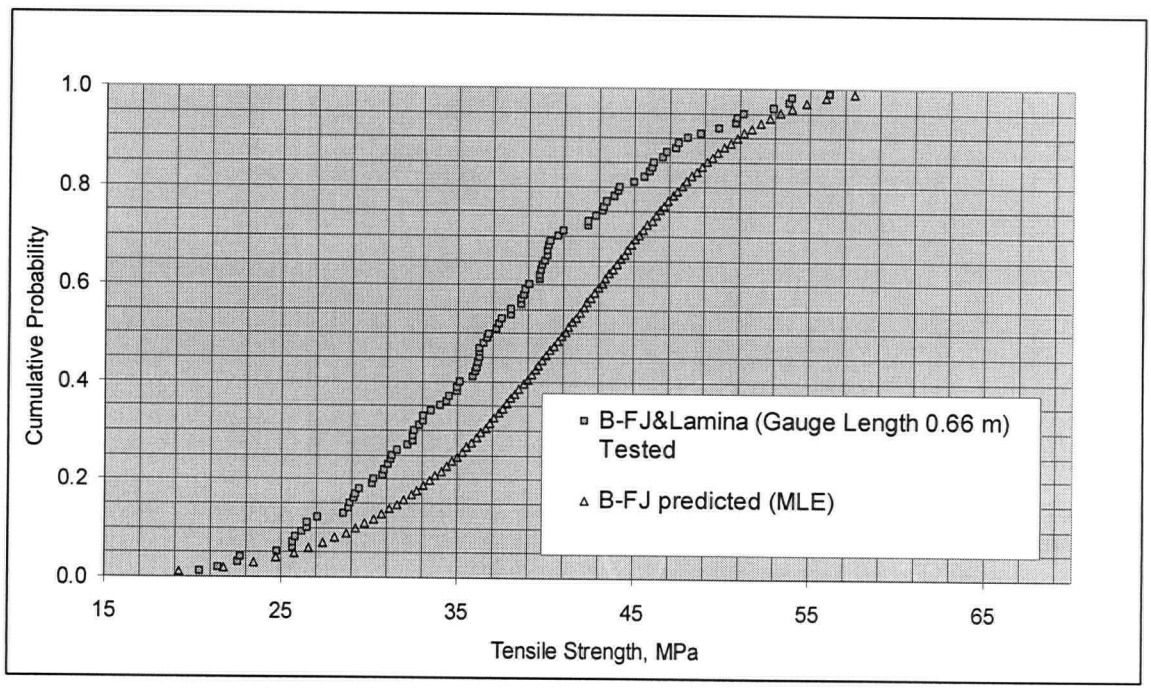

Figure 4.5 Tensile strength distribution of the C grade 38 mm x 140 mm Douglas fir finger joints

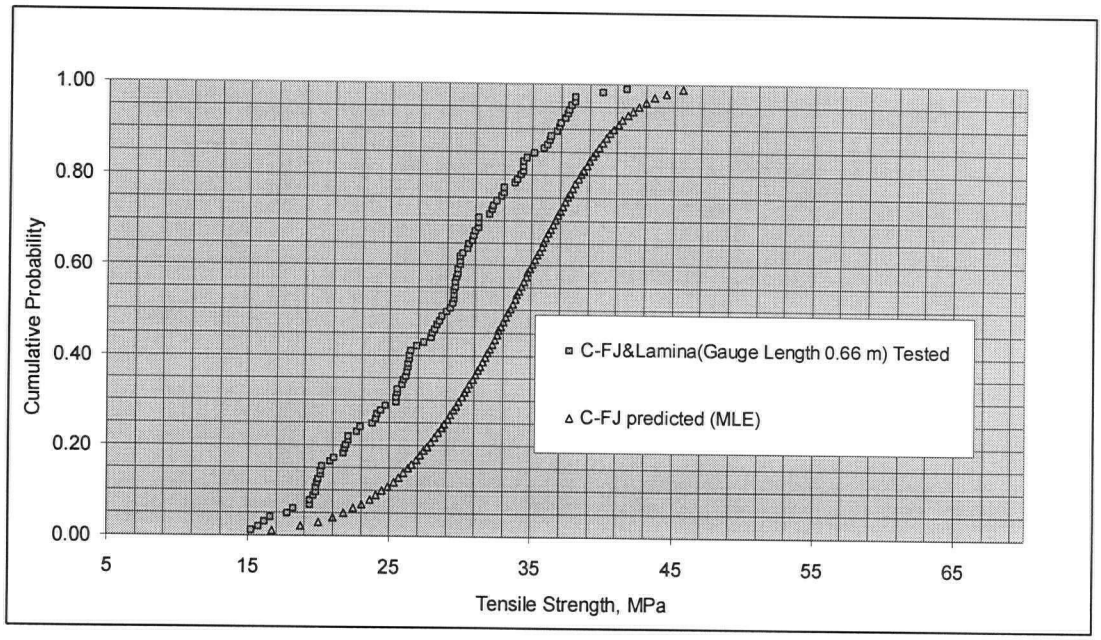

Figure 4.6 Tensile strength distribution of the D grade 38 mm x 140 mm Douglas fir finger joints

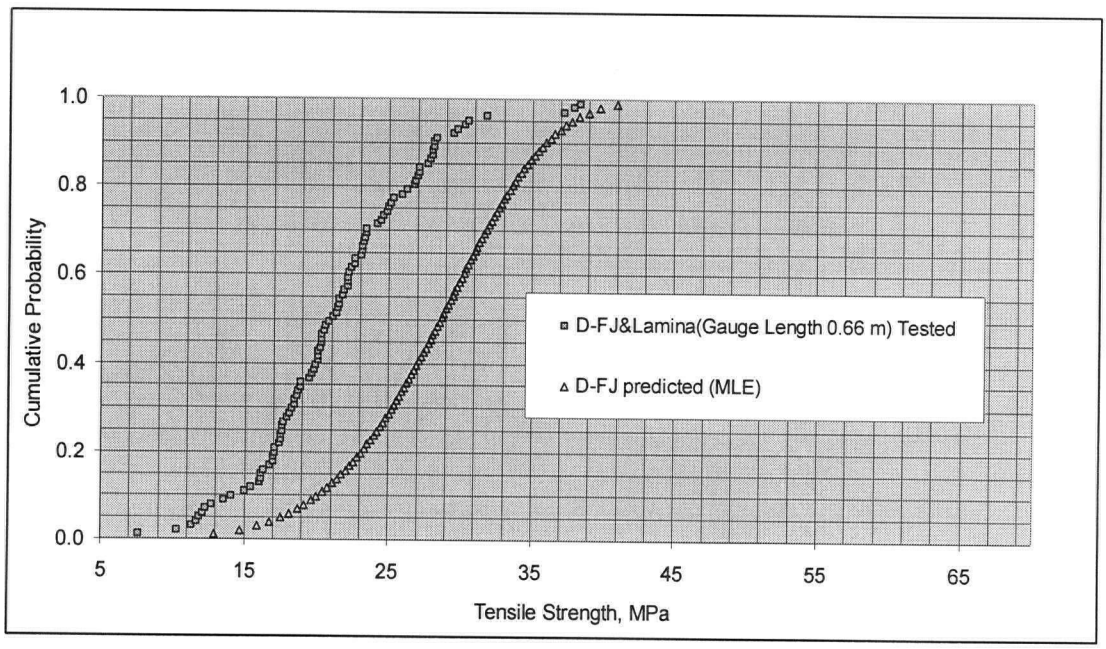

As expected, in T1 grade's case, the lamina strength is much higher than that of the finger joint's. In B grade's case, both strength values come closer and in C grade's and D grade's cases, the finger joint's strength is higher than that of the lamina.

Some of the typical finger joint failure images observed during the laboratory testing is shown in Figure 4.7.

Figure 4.7 Some of the typical finger joint and lamina failures

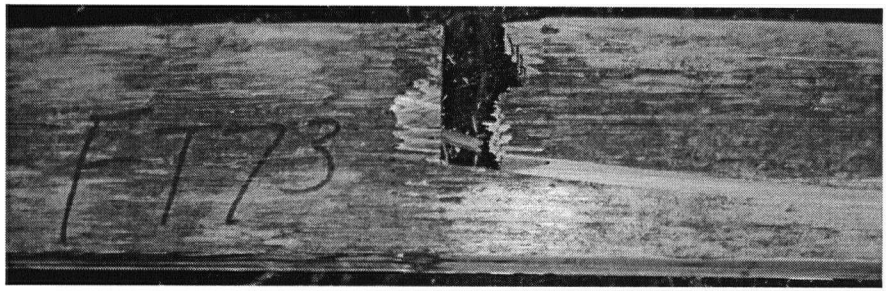

(a)

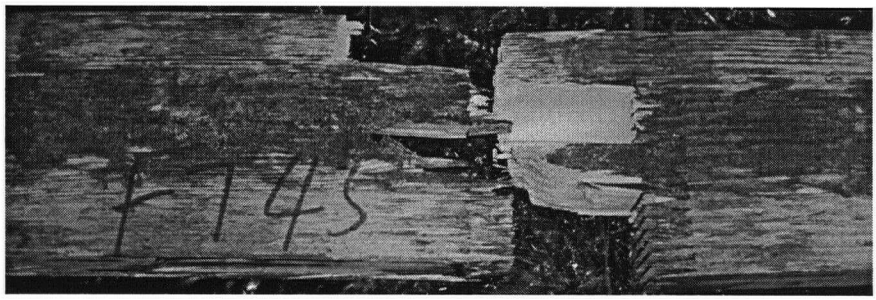

(b)

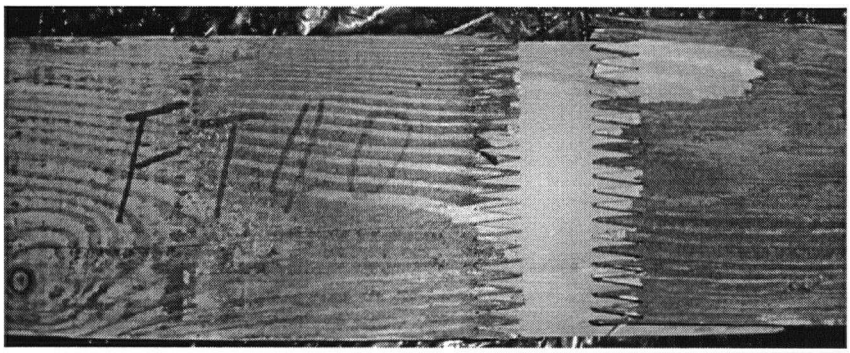

(c)

4.5 MOISTURE CONTENT

Prior to the tensile strength test, all the boards were subjected to moisture content assessment to confirm the acceptable moisture content level of less than 15%. Moisture measurements were taken at three random locations using a moisture meter.

At this stage weight and the dimensions of the specimens were measured to determine the specific gravity of the specimens kept at room temperature. The specific gravity values corresponding to the lamina grades are given in Table 4.5.

Table 4.5 Specific gravity of the new Douglas fir lamina grades measured at test moisture content

Lamina grade	T1	Cc	B	C	D
Mean	0.58	0.56	0.55	0.52	0.50
SD	0.05	0.04	0.04	0.04	0.03

4.6 KNOT SURVEY

The knots present in a wood member are one of the key factors that influence the strength of the member. The size of the knot is measured in terms of the diameter of an equivalent cylinder placed at that section. The size of a knot varies from a tiny pin hole to a size occupying up to 70-80% of the cross-section of the wood. Generally the knots are in conical shape originating from the pith of the wood.

As discussed earlier ASTM D 3737 provides guidelines for knot measurement and the use of knot data to determine the allowable properties of the glue laminated timber beams.

Glulam beam analysis using the GAP program and the knot data were carried out by Dr. Borjen Yeh (APA). In general the GAP program results indicated a satisfactory performance of the proposed grades.

4.6.1 KNOT SURVEY: PROCEDURE

ASTM D3737 requires physical measurements (mapping) of all the knots in individual pieces of lumber. A set of nine types of knots and their measurement procedures are outlined in this standard. Based on the standards, all knots greater than 6 mm of equivalent cylindrical cross-section were measured. A sample consisting of a minimum of 100 pieces or 300 m of lumber randomly chosen from a representative group was considered for the assessment of each grade. The details of the lamina samples used for the knot survey assessments are given in Table 4.6.

Table 4.6 Details of the lamina samples used for the knot survey

Lamina grade	T1	B	Cc	C	D	Total
Total length of lamina, m	419	383	119	885	1,068	2,875

The types of the knots were determined based on the location and the shape of the knot. The measurements of the Types 7 and 8 knots were associated with the location of the pith center (Figure 4.8). Most of the cases, it was inside the lamina and its location

was determined based on the locations /exposures of the pith outcrops. Therefore, generally the values corresponding to the parameters P1 and P2 were estimated based on judgments.

Figure 4.8 Illustration of the pith center of a knot in a cross section of a lamina

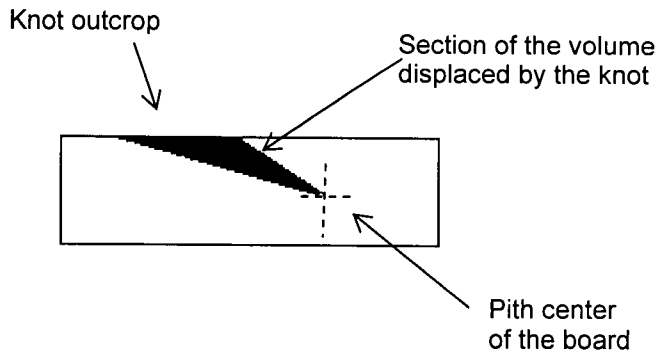

As the standard requires, the scope of the knot survey was to measure all the knots greater than 6 mm. The dimensions of Types 1 and 2 knots were measured quickly; whereas Types 3 and 6 knots took little bit more time to determine some of the dimensions. Therefore, in order to ensure that all the knots greater than 6 mm were measured and expedite the knot survey process, most of the knots having an exposure larger than 6 mm across the lamina were measured with reasonable judgment.

4.6.2 KNOT SIZE CALCULATION

The knot size corresponds to the diameter of the cylindrical section equivalent to the area displaced by the knot. Each of the considered nine basic knot types needs different sets of formulation to calculate their knot sizes. Furthermore within a knot type group, this formulation was slightly different based on the knot's orientation with the reference side of the board. Calculating large number of knot-sizes using simple

manual/measures was practically impossible. Therefore a spread sheet program was developed to track the knot orientation from the knot data and automatically calculate the knot sizes.

4.6.3 RESULTS

Table 4.7 shows the typical distribution of the knot sizes with the lamina grades T1, B, Cc, C and D and Figures 4.9 and 4.10 show the corresponding knot size distributions. The values given in Table 4.8 were normalized corresponding to a lamina length of 300 m per grade for comparison purposes.

Table 4.7 Knot survey summary, details of the knot distribution corresponding to knot size

		Number of knots				
Lamina grades		**T1**	**B**	**Cc**	**C**	**D**
Knot size, K*, cm	**K < 6**	292	267		456	603
	0.6 < K < 1.5	569	826	152	1788	2720
	1.5 < K < 2.5	100	223	81	692	995
	2.5 < K < 3.5	13	37	13	103	153
	3.5 < K			12	31	42
Maximum knot recorded, cm						7.4

**The knot sizes correspond to a single knot and the knot size values were calculated using a spread sheet program.*

Figure 4.9 Knot size distributions

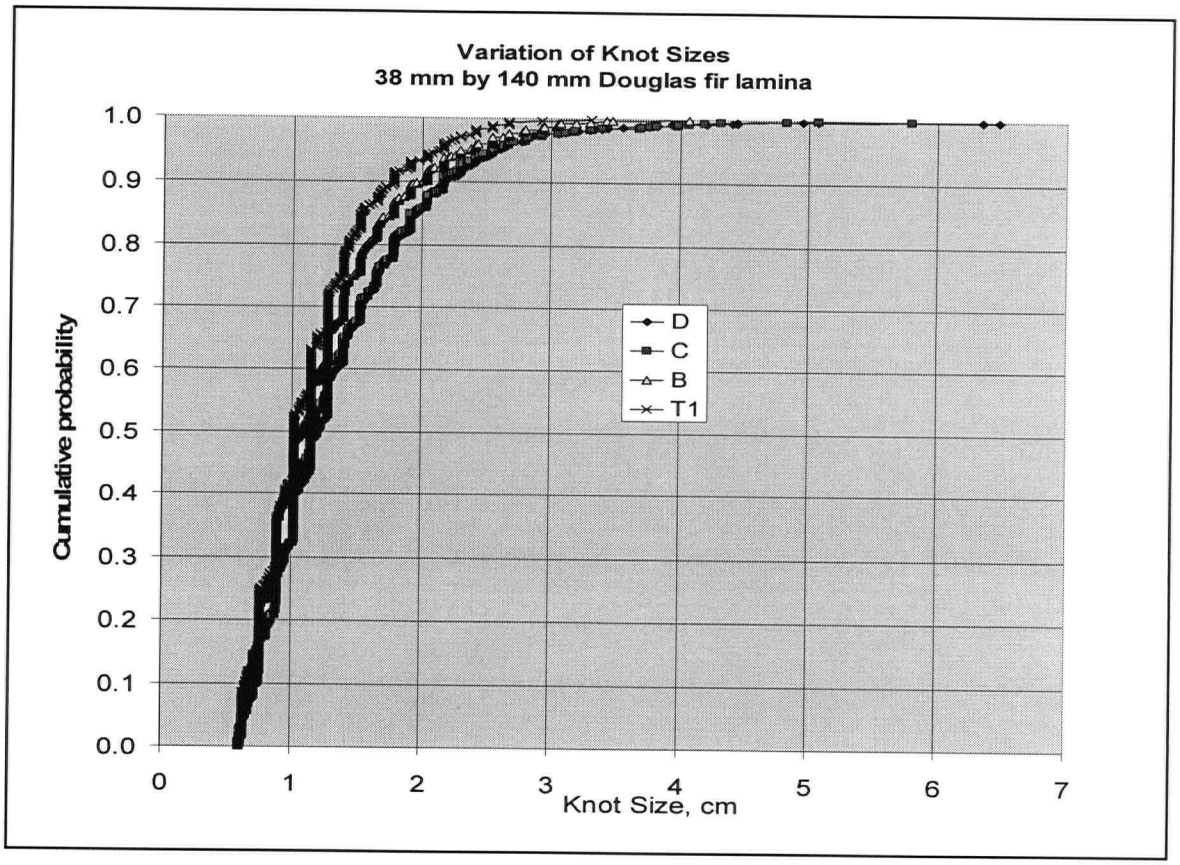

Figure 4.10 Knot size distributions at the upper tail

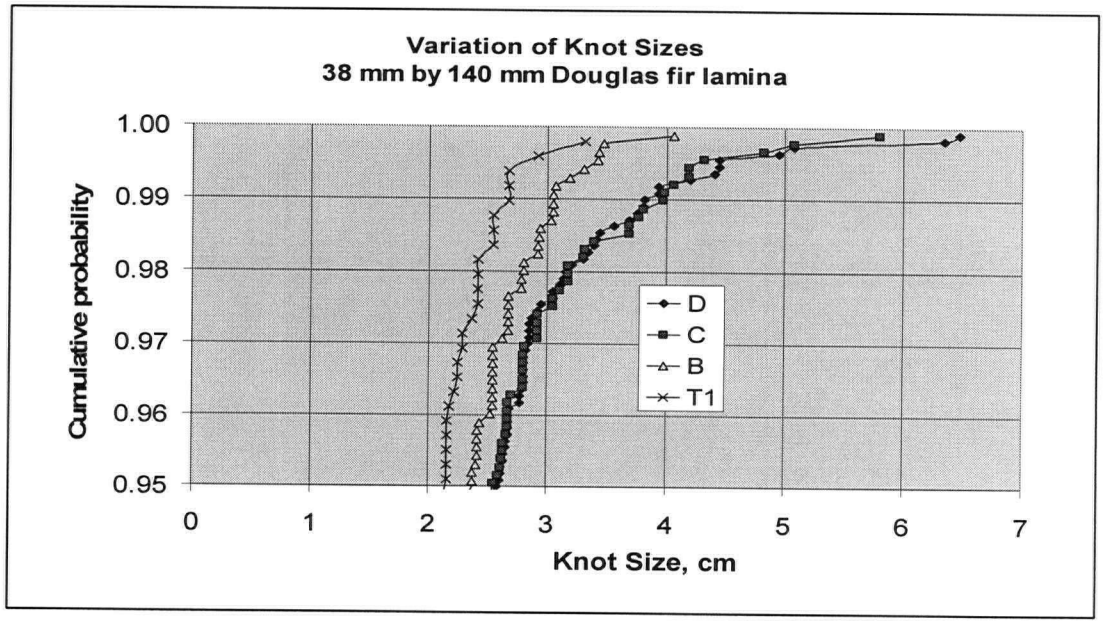

Table 4.8 Knot survey results: Values corresponding to 300 m length of laminae

Lamina grade		Number of knots				
		T1	B	Cc	C	D
Knot size, K, cm	0.6 < K < 1.5	407	647	382	606	764
	1.5 < K < 2.5	72	175	203	235	279
	2.5 < K < 3.5	9	29	33	35	43
	3.5 < K	0	0	30	11	12
Total		488	851	648	886	1098

Chapter 5

Glulam Beam Modeling and Calibration

5.1 INTRODUTION

The beam modeling process deals with two main aspects: fine tuning and validating the ULAG program for glulam strength assessments to confirm code requirements and to assess the performance of the new lamina grades.

First ULAG program itself needs some modifications to make it compatible with the current windows XP versions. Subsequently some additional routines and procedures were introduced into the program to incorporate the shear strength assessments and to account for the laminating factors during the beam simulations as well.

Initially a series of trial ULAG simulations were carried out to study the beam strength characteristics corresponding to different beam lay-ups. This information was used to assess the performance of the new lamina grades and to select the trial laminating factors which were used in subsequent ULAG simulations. Parallel to the ULAG analysis, a set of GAP analysis was carried out by Dr. Borjen Yeh (APA) to confirm the model requirements according to ASTM. Based on these findings beam dimensions and lay-ups for the calibration tests were determined.

Three beam cases, one for bending and two for shear were chosen for the calibration tests. The beams were manufactured in a glulam plant and the testing was carried out at UBC.

5.2 ULAG UPGRADING

The ULAG was originally composed using Lahey FORTRAN, one of the FORTRAN compliers commonly used during mid 1980's. The program needs a re-compiling using one of the latest versions of the FORTRAN complier in order to make it compatible with the current Windows XP platforms.

The re-compiling was carried out using the Digital Visual Fortran software. During the re-compiling process some of the old commands were replaced with the equivalent ones compatible with the Digital Visual Fortran (1988).

5.3 ULAG ANALYSIS

The basic input material for the ULAG analysis were the tensile strength and the MOE test databases of the lamina and finger joints and the length distribution of the lamina. Here the tensile strength and the MOE are provided as a companion data set, based on which the program determines MOE for the boards and the corresponding tensile strength during the beam simulation. The finger joint strength database was developed based on the MLE assessment. The MLE finger joint strength did not have a corresponding MOE values; therefore, a series of MOE values were randomly selected from the lamina-MOE database and used as companion data. A very low correlation is expected between the finger joint strength and MOE data sets.

Other material parameters of interest are the proof load levels of the lamina and finger joints, the minimum permissible MOE values to the beam lay-ups and the laminating factors. The minimum tensile strength values of the lamina and finger joints obtained from the laboratory tests were used as the proof load for each of the lamina

grades considered. The minimum MOE specifications for the T1, Cc, B, and C lamina grades were used as the minimum permissible MOE values in the beam lay-ups. There were no minimum values used for the D grade lamina as there was no minimum value specified for this grade. Furthermore, this is the first time laminating factors were incorporated in the ULAG assessments. A set of four laminating factors for the lamina grades T1, B, C and D were determined based on a trial and error assessment. Then the data was used in all the subsequent ULAG analysis to account for the laminating effects.

During the ULAG assessments, the finite element glulam beam models were simulated with 0.05 m segments along the beam length. The models were subjected to a virtual progressive loading until collapse yielding the corresponding failure load, MOE and the failure details. For each of the beam case investigated, the beam strength statistics were determined based on a set of one thousand beam-simulation and loading data.

The key ULAG assessments were carried out at three stages. Preliminary ULAG simulations were carried out after the tensile strength assessments of laminae and finger joints. The re-complied ULAG program (compatible with the Windows XP platforms) was used for this assessment. This analysis was focused on assessing the performance of the proposed lamina grades and to estimate the corresponding laminating factors. The second stage of analysis focused on determining the beam-lay-ups for the calibration tests. The upgraded ULAG program with the shear strength assessment features and the updated strength database with an additional thirty finger joint test results was used for this assessment. The third step of ULAG analysis concerned with the beam lay-ups and configurations for the glulam verification tests. The finalized ULAG program was used for this assessment.

5.3.1 PERFORMANCE OF THE LAMINA GRADES

Initially a series of trial ULAG assessments were carried out with different beam lay-up arrangements to investigate the performance of the proposed lamina grades. The on hand tensile strength and the MOE values of the lamina grades were used for these assessments. This is a preliminary analysis, intended on identifying the border-line issues, therefore, it didn't include the laminating effects of the glulam lay-up. Details of the beam lay-ups used for this assessment are given in Table 5.1. The results of the corresponding ULAG simulations carried out with 21 span to depth ratio are given in Table 5.2.

Table 5.1 Details of the beam lay-ups used for the initial ULAG simulations

Lamina number (from the bottom of the beam)	Lay-up-ID									
	A1	A1u	A8	A8u	A6	A6u	A9	A9u	A7	A7u
12									T1	Cc
11									B	B
10					T1	Cc	Cc	Cc	C	C
9					B	B	C	C	D	D
8	T1	Cc	T1	Cc	D	D	D	D	D	D
7	B	B	C	C	D	D	D	D	D	D
6	D	D	D	D	D	D	D	D	D	D
5	D	D	D	D	D	D	D	D	D	D
4	D	D	D	D	D	D	D	D	D	D
3	D	D	D	D	D	D	D	D	C	C
2	B	B	C	C	B	B	C	C	B	B
1	T1	T1	T1	T1	T1	T1	T1	T1	T1	T1

Table 5.2 Summary of the preliminary ULAG simulation (bending, 3rd point loading)

		Balanced					Unbalanced				
Beam lay-up, ID		**A1**	**A8**	**A6**	**A9**	**A7**	**A1u**	**A8u**	**A6u**	**A9U**	**A7u**
Beam depth, h, cm		30	30	37.5	37.5	45	30	30	37.5	37.5	45
Beam length, m		6.71	6.71	8.31	8.31	9.91	6.71	6.71	8.31	8.31	9.91
Beam test span, m		6.30	6.30	7.88	7.88	9.45	6.30	6.30	7.88	7.88	9.45
Ultimate failure load, kN	**Mean**	92	87	106	105	119	90	86	105	101	117
	SD	12	11	13	11	14	12	11	13	12	13
MOR, MPa	**Mean**	51	48	47	46	44	50	47	46	45	43
	SD	7	6	6	5	5	6	6	6	5	5
COV, %		13	13	12	10	12	13	13	12	12	11
Specified strength, Rs, MPa		**35**	**34**	**35**	**36**	**34**	**35**	**33**	**34**	**33**	**34**

The specified strength values of these trials are above the target value (30.6 MPa) for the 24f glulam beams. This indicates a satisfactory performance of the proposed lamina grades. The reliability based normalization procedures adopted for the specified strength assessments is discussed in section 5.8.

5.3.2 TENSION LAMINATING FACTORS

As discussed in Chapter 2, laminating factors play a positive role in modifying the strength of the glulam beam. However, so far laminating factors were not considered in the ULAG model.

During the current analysis, it was realized that the relative support from adjacent laminae tends to reduce when the level of strain increases across the beam. Considering this as a basis, a series of ULAG simulations were carried out with different combination of laminating factors ranging from 1.0 to 2.0. Based on this, a trial set of laminating factors were proposed for the new lamina grades (Table 5.3). These factors were used in subsequent ULAG analysis to determine the beam configuration and loading setup for the calibration tests.

Table 5.3 Trial sets of laminating grades proposed for the new lamina grades

Material grade	Laminating factor
T1	1.1
B	1.2
C	1.3
D	1.4

5.3.3 BENDING SIMULATIONS

As mentioned earlier the second stage of the ULAG analysis focused on determining the beam-lay-ups for the ULAG calibration tests. A series of glulam trial bending and shear simulations were carried out to identify the beam lay-up satisfying a 24f 1.8 E grade.

Beam lay-up and dimensions of the finalized beam selected for the bending tests are given in Table 5.4 and the strength parameters predicted prior to the calibration tests are given in Table 5.5.

Table 5.4 Beam lay-ups selected for ULAG calibration (beam ID A8U)

Lamina number (from the bottom of the beam)	1	2	3	4	5	6	7	8
Lamina grades	T1	C	D	D	D	D	C	Cc

Table 5.5 ULAG strength predictions for the trial beams

Lay-up ID		A8U
Beam depth, m		0.30
Test span, m		6.40
Ultimate failure load	Mean, kN	88.9
	COV, %	14
MOR	Mean, MPa	49.0
Specified strength, MPa		34.5

5.4 ULAG CALIBRATION TESTS – FLEXURE

A set of twenty-four 0.30 m deep glulam beams manufactured according to the beam lay-up proposed based on the ULAG simulations (Tables 5.4 and 5.5) were used for the bending calibration tests. The tests were carried out with a third point loading (Figures 5.1 and 5.2, Table 5.6).

The test apparatus consists of two end supports, two loading heads attached to a load evener and a machine head. The advancement of the machine head and the corresponding load is monitored and controlled by a computerized data acquisition system. The beams were tested with 21 span to depth ratio. The loading rate was kept at

10 mm/ min to maintain an average failure time of 10 minutes. All the beam tests were videotaped.

Figure 5.1 Typical third point loading configuration used for the bending test

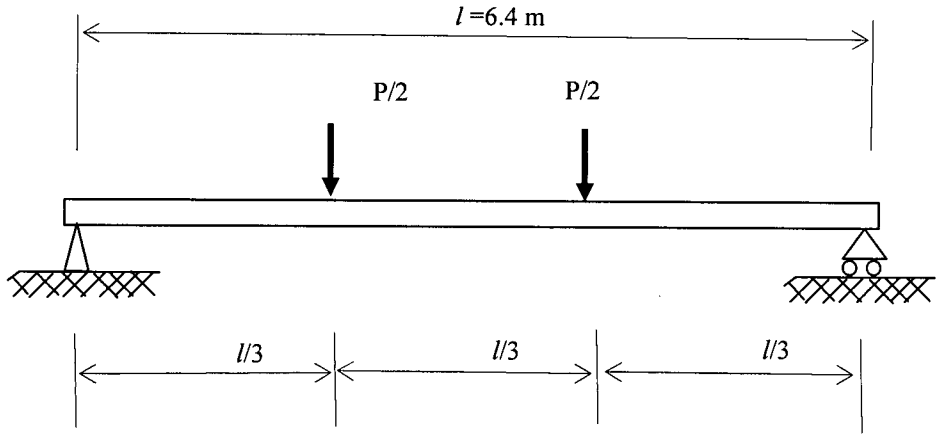

l - test span
P- total load on the beam

Table 5.6 Details of the bending test configuration

Beam set ID	E
Beam depth	0.30 m (1 ft)
Beam width	0.130 m (5 ¼ in.)
Span to depth ratio	21
Test span	6.40 m (21 ft)
Beam length	6.71 m (22 ft)
Loading rate	10 mm /min

Figure 5.2 Test setup for the 0.30 m deep beam

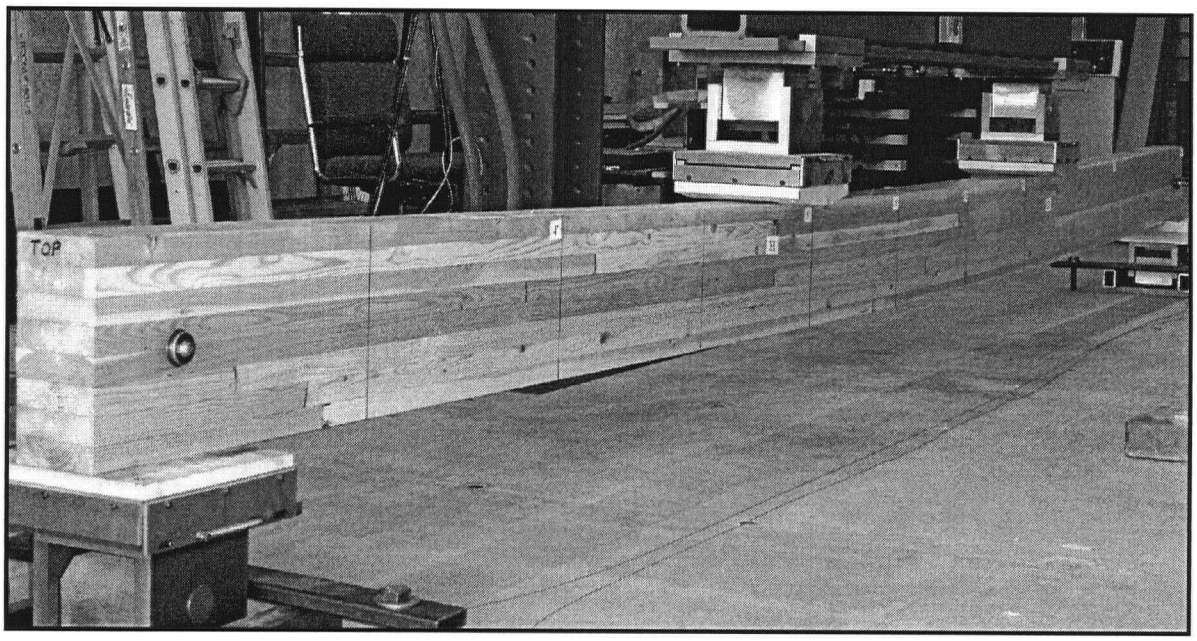

The summary of the bending test results is given in Table 5.7 and a comparison between the ULAG predicted strength distribution and the laboratory test results are given in Figure 5.3.

Table 5.7 Summary of the bending test results

Beam depth, m		0.30
MOR	**Mean, MPa**	48.3
	COV, %	11
Specified strength, MPa		34.5

Figure 5.3 Comparison between the ULAG predicted strength distribution and the laboratory test results for 0.30 m deep glulam beams

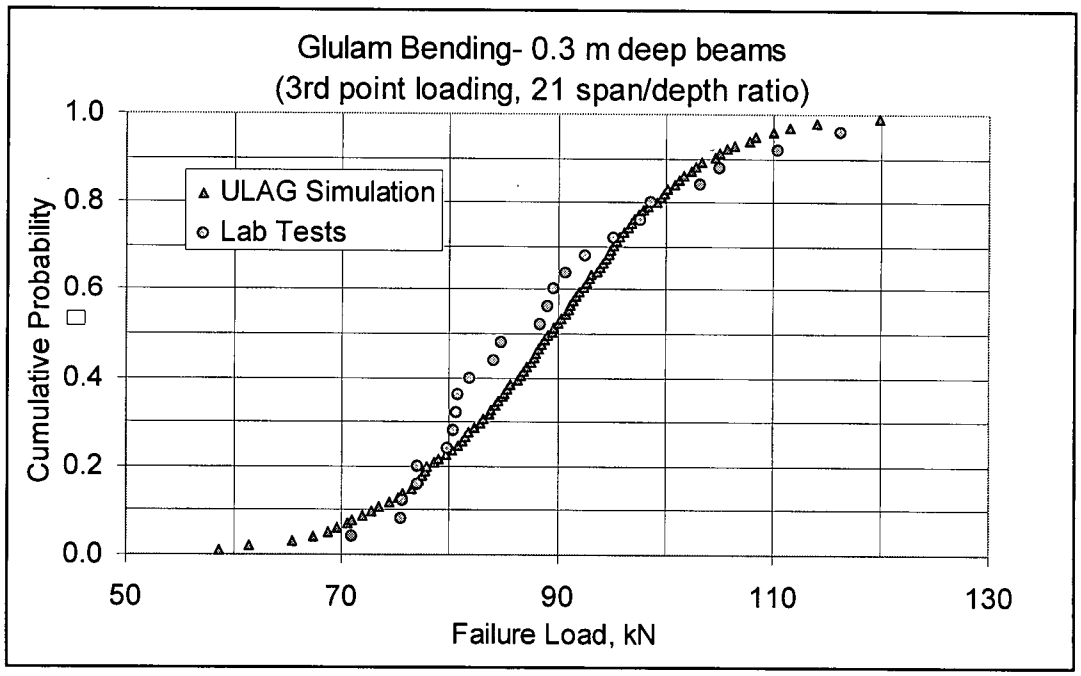

The details of key failures observed during the glulam bending tests are given in Table 5.8.

Table 5.8 Key failures observed in 0. 30 m deep beams

Failure type	Number of breakdowns
finger joint	8
finger joint and knot	5
finger joint and lamina	4
lamina	6
slope of grain (SOG) and knot	1

An image of one of the bending failures case is shown in Figure 5.4.

Figure 5.4 Bending failure of a 0.30 m deep glulam beam

5.4.1 MOE VALUES

MOE values for all the bending beams were evaluated from load-deformation curves obtained prior to the ultimate loading. A specially designed cable yoke system as shown in Figure 5.5 was used to obtain the required load-deflection data with a loading level of 25% of the ULAG predicted mean failure load. This cable system consists of a cable (Air craft cable, 1.58 mm diameter and maximum working load capacity of 43 kg), pair of pulleys, a weight (4.5 kg) and a displacement-gauge connected to the data acquisition system. The pulleys were fixed on the vertical face of the beam, at the intersection of the simple support reaction line and the horizontal axis of the beam. Then the cable was fitted over the pulleys to form a loop. The constant weight was applied at the center of the lower portion of the cable to keep the upper portion of the cable taut. The slope of the lower portion of the cable was kept around 10 degrees and a load in the range between 200 N to 250 N was expected on the cable. The vertical relative displacement between the upper portion of the cable and the horizontal axis of the beam

was measured at the middle of the beam during loading. This value corresponds to the relative displacement of the beam at the given load level.

Figure 5.5 Cable - yoke system used to measure the relative displacement at the middle of the beam

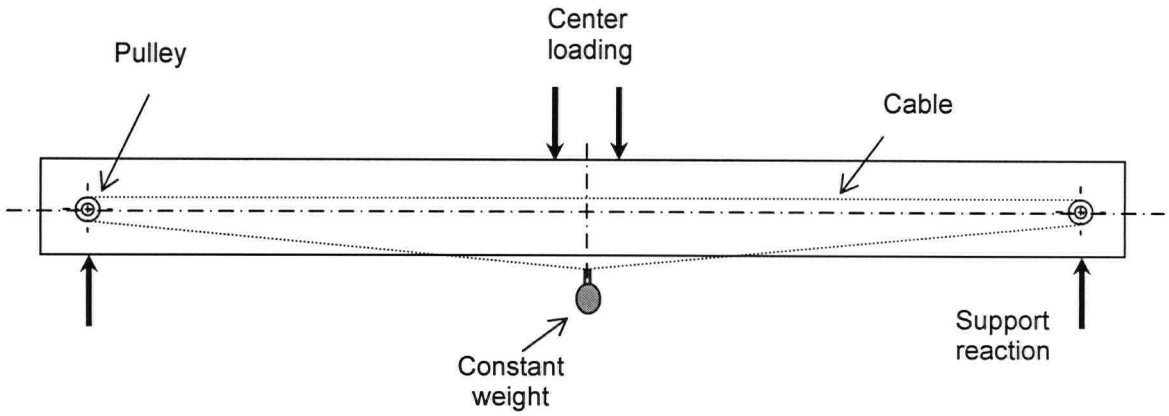

The summary of the MOE value for the 0.30 m deep bending beam is given in Table 5.9.

Table 5.9 Summary of the MOE values of the 0.30 m deep bending beams

Parameter	MOE values
Mean, MPa	13,326
COV, %	4

5.4.2 ULAG CALIBRATION (BENDING)

A comparison of the specified strength and mean modulus of elasticity values based on the bending test results and the ULAG predictions made prior to the calibration tests are given in Tables 5.10 and 5.11, respectively.

Table 5.10 Comparison between bending test results and ULAG prediction – specified strength

Beam case	Glulam specified strength		
	Based on laboratory test results (MPa)	Based on ULAG simulations (MPa)	Error %
0.31 m deep beam at 21 span/depth ratio	34.5	34.5	-0.2

Table 5.11 Comparison between bending test results and ULAG prediction – MOE

	MOE_{mean}		
Beam case	Based on laboratory test results (MPa)	Based on ULAG simulations (MPa)	Error %
0.30 m deep beams at 21 span/depth ratio	13,326	12,484	-6.3

A very small -0.2 % error was observed for the glulam specified strength prediction. The corresponding error for the mean MOE prediction is -6.3%. These errors are within the acceptable limit. Therefore, at this stage no further modifications or fine tuning is required in either the ULAG model or the proposed laminating factor set.

5.5 ULAG SHEAR

As part of the ULAG upgrading process new routines were introduced in the ULAG model to incorporate additional features needed to investigate shear failures. A finite element model volume integrating scheme of Foschi & Barrett (1976) and Lam et al. (1997) was used for this assessment. This model basically predicts the failure load of a full scale beam that has a common probability of failure as a clear wood block shear specimen.

5.5.1 NUMERICAL MODELING

The following section summarizes the numerical formulation of the shear stress assessment procedures.

The displacement field of the beam-column element is given by :

$$U = N\,d \qquad (5.1)$$

where $u \equiv [\,u, \varphi, w]^t$, $d \equiv [\,u_1, \varphi_1, w_1, \theta_1, u_2, \varphi_2, \theta_2]^t$ and $N \equiv$ shape function array.

u and w denote, respectively the axial and transverse displacements of the beam-column axis, φ is the rotation of a transverse normal about this axis, and θ_i is the variation of w_i with respect to the principal bending axial coordinate x for i = 1, 2.

For a given beam lay-up, the nodal displacements d_i (i = 1, 2 , number of nodes) can be determined using the existing ULAG program and therefore, the displacement field U can be evaluated.

Now the transverse shear strain γ ($\gamma << 1$) can be given by the following equation :

$$\gamma = \left(\varphi + \frac{dw}{dx}\right)\left[1 - 4\left(\frac{z}{h}\right)^2\right] \qquad (5.2)$$

where, z is the thickness coordinate and h is the height of the beam.

Then the shear stress developed for a given load level can be determined based on the following equation:

$$\tau = G\,\gamma \qquad (5.3)$$

The values of the shear modulus G is generally given as a ratio of MOE (E/G ratio). The typical E/G ratio of 20 is used in the current analysis.

Now, based the weakest link theory (Foschi and Barrett, 1976) the mean shear failure load P can be written as :

$$P = \frac{P\tau^*_{0.5}}{I^{1/K}} \qquad (5.4)$$

where,

$\tau^*_{0.5}$ - mean shear strength of a unit volume 1.64E-05 m^3 (1 $in.^3$)

I - shear stress field integrated over the volume under the applied load P

k - Weibull shape parameter.

$\tau^*_{0.5}$ can be determined based on the following relationship (Foschi and Barrett 1976) :

$$\tau^*_{0.5} = \beta_t \tau_{ASTM} \qquad (5.5)$$

where,

$$\beta_t = 1.333+0.336(k-4) \qquad if\ 4 \le k \le 8$$

$$\beta_t = 2.678+0.251(k-8) \qquad if\ 8 \le k \le 10$$

τ_{ASTM} is the ASTM block shear strength at the probability of interest.

5.5.2 SHEAR SIMULATIONS

The main aims of the shear analysis are to determine a beam configuration which will be more vulnerable to shear failure and to identify the ultimate loading level. In general the chances of getting pure shear failure can be increased by reducing the beam test span under a simple three point loading. However, there are many practical issues to account for when designing the beams for shear test. At very short span, the ultimate failure load levels are expected to be very high. High load level may cause crushing or excessive deformation near the loading head and supports. Also it requires a higher-capacity testing facility to safely handle these extraordinary loads. Therefore, the target is to produce a significant number of shear failures with a moderate load level and determine the overall shear strength parameters using the maximum likelihood method (MLE).

The clear wood-shear strength parameters (Table 5.12) reported by Lam et al. (1997) was used as basis for the clear wood strength corresponding to the D grade Douglas fir material. The beam-lay-up given in Table 5.13 was used for this assessment.

Table 5.12 Clear wood Douglas fir shear strength (Lam et al. 1997) of a standard block shear

Parameter	τ_{ASTM}
Mean, MPa	8.98
COV, %	16

Table 5.13 Shear calibration beam lay-up (A1)

Lamina number (from the bottom of the beam)	8	7	6	5	4	3	2	1
Lamina grades	T1	B	D	D	D	D	B	T1

Initial simulations were carried out using the clear wood strength parameters given in Table 5.12. The results of these shear assessments are given in Table 5.14.

Table 5.14 Results of the initial shear simulations

Beam depth, m	Span to depth ratio	Predicted shear capacity, kN	Predicted shear strength, MPa
0.30	7	345	6.21
0.30	6	433	7.79

The D grade material used in the glulam shear zone (middle core of the beam) is the weakest grade, expected to be having inferior strength parameters. Therefore, the clear wood strength corresponding to the Douglas fir D grades should be weaker than that of given in Table 5.12. In this way the predicted strength values given in Table 5.14 can be considered as an upper bound for the shear capacity of the glulam beams considered.

5.6 SHEAR TESTS

Two sets of 0.30 m deep glulam beams were tested with two different span to depth ratios 7 and 6 for the shear calibration. Each of these sets consists of 24 beams.

The details of the test configuration used for the shear tests are given in Table 5.15 and the schematic diagram of the typical shear testing arrangement used is shown in

Figure 5.6. This four point loading setup is basically a modified version of the simple three point loading setup used to generate high shear stress at the middle core of the beam. In order to avoid the excessive load concentration at the loading point the center point load was split and applied symmetrically at two locations close to the center.

Table 5.15 Shear test configuration

Beam depth	0.30 m (1 ft)	0.30 m (1 ft)
Beam width	0.129 m (5 ¼ in.)	
Span to depth ratio	7	6
Test span, *l*	2.13 m (7')	1.83 m (6')
Beam length	2.44 m (8')	2.13 m (7')
Loading type	Four point loading	

Figure 5.6 Configuration of the typical shear testing arrangement

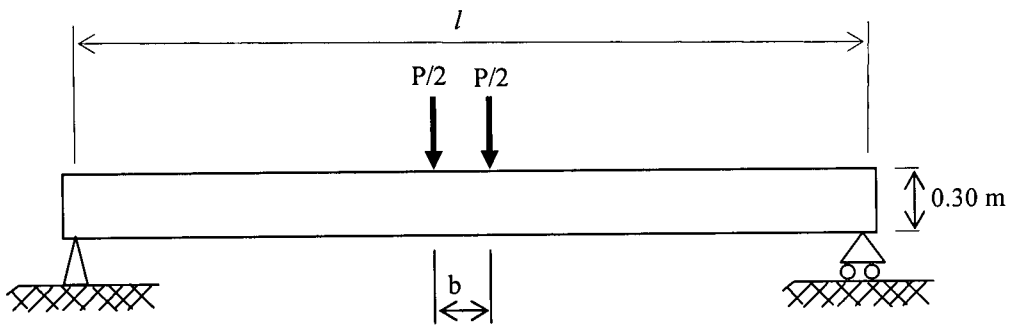

l - test span
b = 0.46 m, the spacing between the pair of loading heads at the center
P- total load on the beam

The summary of the shear test results is given in Table 5.16. This data was processed using the MLE technique in order to determine the uncensored statistical parameters. The MLE predicted 2p-Weibull data and the equivalent normal distribution values are given in Table 5.17 and the corresponding shear strength values are given in Table 5.18.

Table 5.16 Summary of the shear test results

Shear testing case	Failure load		Number of shear failures	Total number of beams tested
	Mean (kN)	COV (%)		
0.30 m deep beams tested at 6 span to depth ratio	311	9	20	24
0.30 m deep beams tested at 7 span to depth ratio	263	10	17	24

Table 5.17 Details of the MLE simulated shear capacity (based on laboratory test results)

Shear testing case	Scale, m (kN)	Shape, k	Mean, (kN)	COV (%)
0.30 m deep beams tested at 6 span to depth ratio	330	9	313	13
0.30 m deep beams tested at 7 span to depth ratio	284	16	275	8

Table 5.18 Shear strength parameters based on the experimental data

Shear testing case	Mean, (MPa)	COV, (%)
0.30 m deep beams tested at 6 span to depth ratio	6.0	13
0.30 m deep beams tested at 7 span to depth ratio	5.3	8

5.6.1 MOE VALUES

For the case of the shear beams, shear deformation is expected to be significant; therefore, MOE values were not measured during the laboratory assessments.

5.6.2 SHEAR FAILURE CHARACTERISTICS

The shear failures of the beams were recognized by a horizontal tearing with an outward jerking of the top portion at one of the end of the beam. Generally the splitting extends up to the mid section. Figure 5.7 shows the end section of a failed shear beam. Here the failure paths can be easily tracked by the breaks in the vertical lines drawn onto the beam surface prior to loading.

Figure 5.7 End section of a failed shear beam
(This beam was 0.30 m deep and tested at 2.13 m test span)

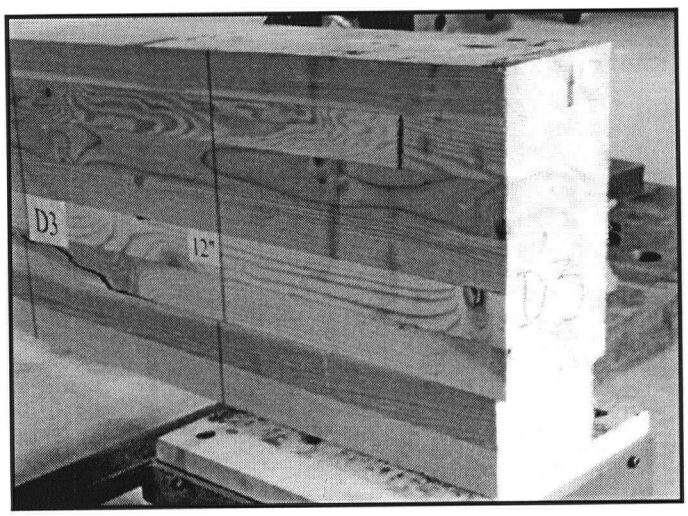

5.6.3 SHEAR CALIBRATION

After the shear beam testing the clear wood strength parameters used in the shear-stress volume model were fine-tuned based on the test results. This was done by a series

of trial and error assessments using different sets of the clear wood strength parameters which are close to the values given in Table 5.12. The selected clear wood strength set which produce the minimum errors between the tested and predicted average shear loads is given in Table 5.19. This is the predicted clear wood strength values for the Douglas fir D grade material.

Table 5.19 Predicted clear wood shear strength values corresponding to Douglas fir D grade laminae.

Parameter	τ_{ASTM}
Mean, MPa	9.0
COV, %	18.0

The results of this analysis with a comparison of the shear test results are given in Table 5.20.

Table 5.20 Predicted shear capacity of the glulam beams

Beam depth, m	Span to depth ratio	Simulated shear capacity, kN	Simulated shear strength, MPa	Tested shear strength, MPa	Error, %
0.30	7	266	5.1	5.3	-3.4
0.30	6	330	6.3	6.0	5.4

5.7 GAP ASSESSMENTS

As mentioned earlier the gap assessments on the new lamina grades were carried out by Dr. Borjen Yeh (APA). The assessments were carried out based on the knot

distribution of the new lamina grades (section 4.6). The laminae lay-ups used for the assessments are given in Table 5.21.

The program predicts the allowable strength capacities equivalent to a standard glulam beam of o.3 m (1 ft.) with 6.4 m (21 ft.) loading span. Corresponding specified strength values and some details of the adjustment carried out to derive that are given in Table 5.22.

Table 5.21 Glulam lay-ups used for the GAP assessments

Lamina number (from the bottom of the beam)	Beam lay-up cases						
	#1(8)	#4(8)	U1(10)	U2(10)	U1(20)	U2(20)	#4(20)
20					Cc	Cc	Cc
19					Cc	Cc	Cc
18					Cc	C	Cc
17					C	C	C
16					C	C	C
15					D	D	D
14					D	D	D
13					D	D	D
12					D	D	D
11					D	D	D
10			Cc	Cc	D	D	D
9			Cc	C	D	D	D
8	Cc	Cc	C	C	D	D	D
7	C	C	D	D	D	D	D
6	D	D	D	D	D	D	D
5	D	D	D	D	C	C	C
4	D	D	D	D	C	C	C
3	D	D	C	C	B	C	B
2	B	C	B	C	T1	T1	B
1	T1	T1	T1	T1	T1	T1	T1

Table 5.22 Details of the specified strength values corresponding to the GAP predicted allowable strengths

Parameters	Beam lay-up cases						
	#1(8)	#4(8)	U1(10)	U2(10)	U1(20)	U2(20)	#4(20)
Depth, m	0.30	0.30	0.38	0.38	0.76	0.76	0.76
Width, m	0.13	0.13	0.13	0.13	0.13	0.13	0.13
No. of laminations	8	8	10	10	20	20	20
Allowable strength predicted by GAP, MPa	18	17	18	17	18	18	18
$MOR(5\%)_{(standard\ beam,\ ASTM)}$, MPa	37	36	37	35	39	38	37
$COV_{(MOR)}$, (assumed same as the corresponding ULAG simulated COV values)	0.17	0.17	0.16	0.16	0.13	0.13	0.14
B (reliability based normalization procedure)	1.15	1.13	1.16	1.17	1.20	1.20	1.20
C_f (tolerance limit), n=50	0.94	0.93	0.94	0.94	0.95	0.95	0.95
Duration of load	0.87	0.87	0.87	0.87	0.87	0.87	0.87
Kz (size adjustment to 0.130 x 0.61 x 9.1 cu. meter)	1.06	1.06	1.06	1.06	1.06	1.06	1.06
Specified strength, $GAP_{(0.13 \times 0.61 \times 9.1\ cu.\ meter)}$, MPa	32.8	31.2	33.3	31.8	36.0	35.1	34.5

Parallel to these GAP analyses a set of ULAG simulations were carried out to assess the performance of the same lay-ups at a span to depth ratio of 15. The ULAG and GAP predicted specified strength values adjusted to the standard beam size of 0.13 x 0.61 x 9.1 cu. meter are compared in Table 5.23.

Table 5.23 Comparison between the ULAG and GAP predicted specified strength values

Parameter	Beam lay-up cases						
	#1(8)	#4(8)	U1(10)	U2(10)	U1(20)	U2(20)	#4(20)
Specified strength, GAP, MPa	32.8	31.2	33.3	31.8	36.0	35.1	34.5
Specified strength, ULAG, MPa	30.1	28.3	32.8	32.6	35.3	35.2	32.8
Ratio of specified strength(ULAG) to specified strength(GAP)	0.92	0.91	0.98	1.03	0.98	1.00	0.95

The GAP predicted specified strength values are above 30.6 MPa. This indicates a satisfactory performance for all the lay-ups considered. The ULAG simulated specified strength values for the 0.3 m deep beam cases #1(8) and #4(8) are below 30.6 MPa. However, #4(8) lay-up simulated at 21 span to depth ratio predicts 34.5 MPa specified strength (Table 5.5 lay-ups A8U and #4(8) are the same). With subsequent investigations it was observed that the ULAG simulated specified strength values tend to decrease with the reduction of the loading span of the beam. Further investigation on this issue to verify these results is recommended.

5.8 DETERMINATION OF SPECIFIED STRENGTH

The Canadian standard specifies the bending, compression and horizontal shear capacities of the glulam beam in terms of the specified strength. This is a modified version of the characteristic strength (5% strength) after the accounting for the reliability factors, duration of load, data confidence and beam size. The details of the assessment of correction factors and the specified strength are discussed below.

The nominal strength R_n can be written as

$$R_n = BR_{0.05}$$

$R_{0.05}$ is the non parametric fifth percentile short term strength.

B is the reliability normalization factor.

$B = 1.58 - 2.18V$ and V is the coefficient of variation.

Data confidence factor C_f is given by, $C_f = 1 - \frac{2.7V}{\sqrt{n}}$ and n is the sample size.

A = 0.87 duration of load factor (Clause 4.3.2 CSA 086-01).

Size factor K_Z is given by $K_Z = 1.03(bL)^{-0.18}$ where b width of the widest building block used in the beam and L is the beam span. This size adjustment is used to correct the strength of the beam considered based on the strength of a standard beam of 0.13 x 0.61 x 9.1 cu. meter.

Based on these correction factors the specified strength (R_S) can be written as given below.

$$R_s = \frac{AC_f R_n}{k_Z} \qquad (5.6)$$

Chapter 6

Glulam Model Verification

6.1 INTRODUCTION

Model verification tests have two main aims, verifying the ULAG prediction and qualifying the proposed lamina-lay-up for the target glulam beam grade. Two sets of glulam beams with depths 0.61 m and 0.45 m were used for the bending and shear verification tests, respectively. Here again the beam depths were chosen based on the ULAG simulations. One of the concerns in selecting the beam depth was to verify the model predictions at significantly different load-levels than that of the calibration test loads. For each case, similar to the calibration tests, twenty four glulam beams manufactured in a glulam plant were used for the assessments and all the testing were carried out at UBC. In both cases the basic loading configuration was kept similar to that of the calibration tests, the bending tests were carried out with third point loading and the shear tests were carried out with a four point loading. The span to depth ratios corresponding to the bending and shear tests were kept at 18 and 6, respectively. These setups were chosen to enhance the breaking at the target failure mode. For each of the test cases different loading rates were used to maintain an average failure time of 10 minutes.

All the beam tests were videotaped and for bending tests and 0.46 m deep shear case high speed video taken at 1000 images per second speed was used to study and detect the failure modes.

6.2 BENDING TESTS

The detail of the test setup and the beam lay-up used for the assessment are given in Tables 6.1 and 6.2. The bending verification beams are fairly deep beams. Therefore, four special lateral supports were provided at 1.22 m, 2.74 m, 8.53 m and 10.06 m locations to provide support against lateral instability.

Figure 6.1 Typical third point loading configuration used for the bending test

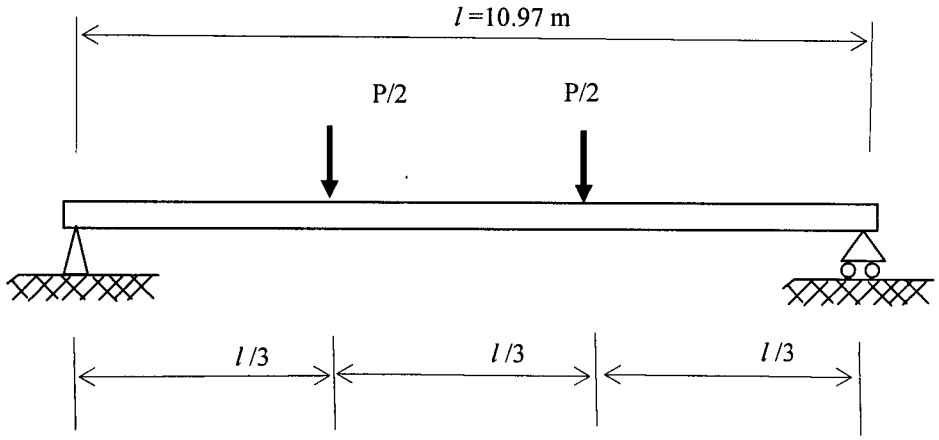

l - test span
P - total load on the beam

Table 6.1 Details of the bending test configuration

Beam case	**F**
Beam depth	0.61 m (2 ft)
Beam width	0.130 m (5 ¼ in.)
Span to depth ratio	18
Test span, *l*	10.97 m (36 ft)
Beam length	11.28 m (37 ft)
Loading rate	13 mm/min

Table 6.2 Beam lay-ups selected for bending tests (beam ID A5U)

Lamina grades	1	2	3	4	5	6	7	8	9	10	11	12	13	14	15	16
Lamina number (from the bottom of the beam)	T1	B	C	C	D	D	D	D	D	D	D	D	C	C	B	Cc

Figure 6.2 Test setup for the 0.61 m deep glulam bending beam

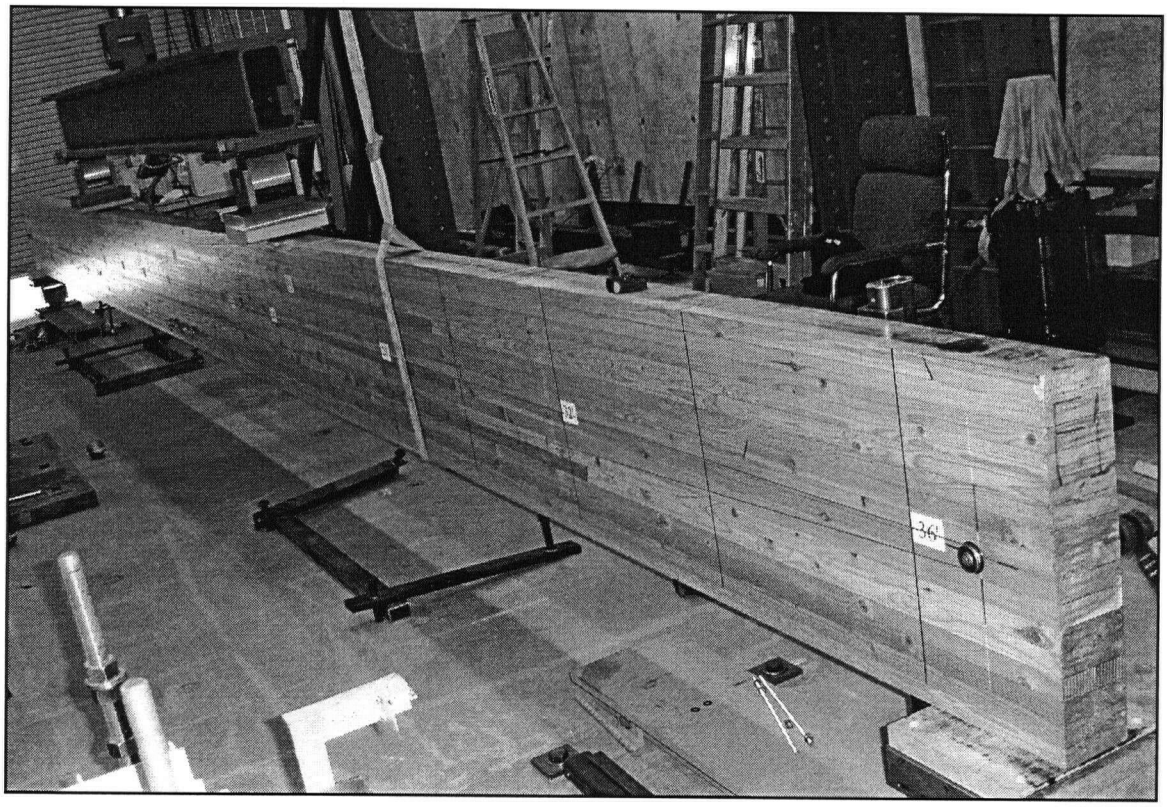

The summary of the bending test result is given in Table 6.3 and a comparison between the ULAG predicted strength distribution and the laboratory test results are given in Figure 6.3.

Table 6.3 Summary of the bending test results

Beam depth, m		0.61
MOR	Mean, MPa	41.8
	COV, %	14
Specified strength, MPa		32.2

Figure 6.3 Comparison between the ULAG predicted strength distribution and the laboratory test results for 0.61 m deep glulam beams

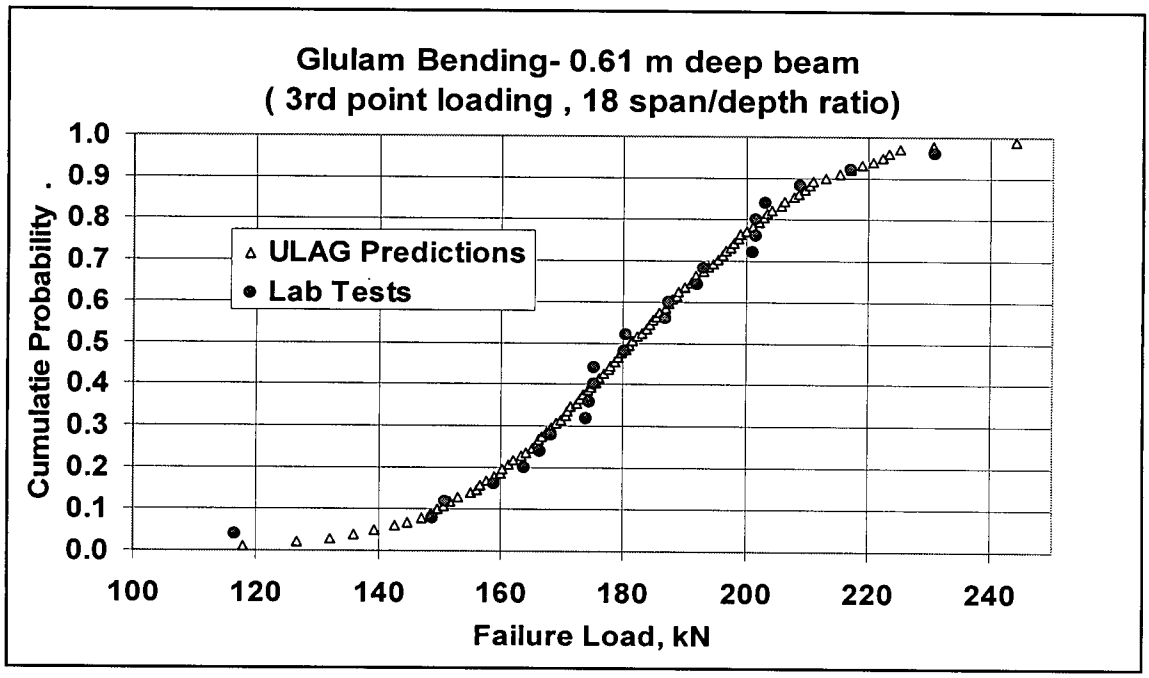

The details of key failures observed during the glulam bending tests are given in Table 6.4.

Table 6.4 Key failures observed in 0.61 m deep beams

Failure type	Number of breakdowns
finger joint	14
finger joint and lamina	1
finger joint and knot	1
knot	1
knot, SOG and lamina	1
lamina	3
lamina and finger joint	1
shake	1
SOG	1

Images of two of the bending failures are shown in Figures 6.4 and 6.5.

Figure 6.4 Bending failure of a 0.61 m deep glulam beam

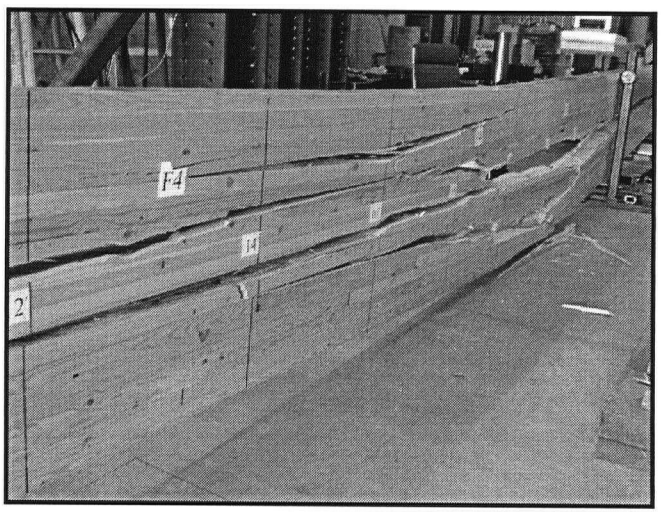

Figure 6.5 Bending failure of a 0.61 m deep glulam beam

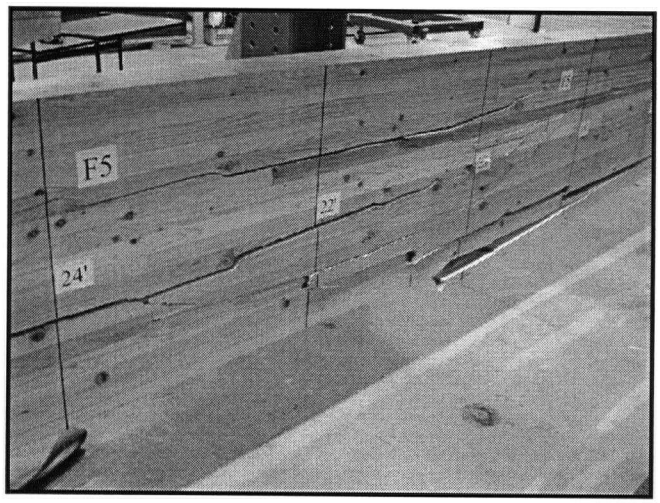

6.2.1 MOE VALUES

MOE values for all the bending beams were evaluated from load-deformation curves obtained prior to the ultimate loading. A specially designed cable yoke system similar to the one used in the calibration test was used to track the beam deflections.

The summary of the MOE values for the 0.61 m deep bending beams are given in Table 6.5.

Table 6.5 Summary of the MOE values of the 0.61 m deep bending beams

Parameter	0.61 m deep beams
Mean, MPa	12,923
COV, %	3

6.3 SHEAR TESTS

As mentioned earlier twenty four 0.46 m deep shear beams at 6 span to depth ratio was used for the assessments.

The details of the test configuration used for the shear tests are given in Table 6.6 and the schematic diagrams of the typical shear testing arrangements used are shown in Figure 6.6. Similar to the shear calibration tests, four point loading setup was selected to avoid the excessive load concentration at the loading point.

Table 6.6 Shear test configuration

Beam depth	0.45 m (1.5 ft)
Beam width	0.13 m (5 ¼ in.)
Span/depth ratio	6
Beam length	3.1 m (10 ft and 2 in.)
Test span, *l*	2.74m (ft)
Loading type	Four point loading

Figure 6.6 Configuration of the typical shear testing arrangement

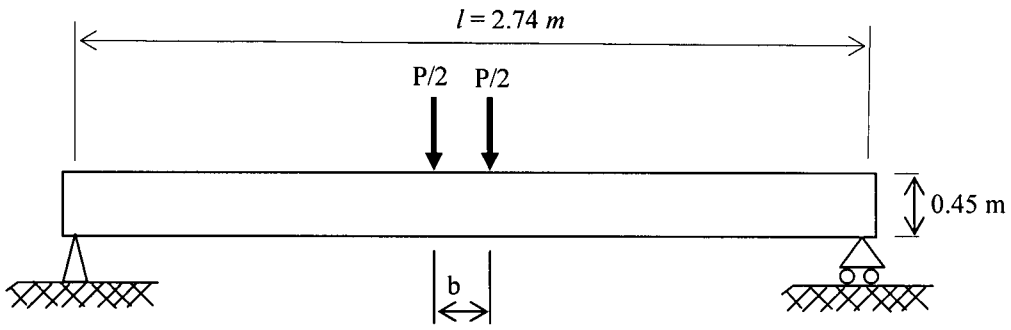

l - test span
P – total load on the beam
b = 0.46 m, spacing between the pair of loading heads at the center.

The summary of the shear test results is given in Table 6.7. This data was processed using the MLE technique in order to determine the uncensored statistical parameters. The MLE predicted 2p-Weibull data and the equivalent normal distribution values are given in Table 6.8 and the corresponding shear strength values are given in Table 6.9.

Table 6.7 Summary of the shear test results

Shear testing case	Failure load		Number of shear failures	Total number of beams tested
	Mean (kN)	COV (%)		
0.46 m deep beams tested at 6 span to depth ratio	389	10	18	24

Table 6.8 Details of the MLE simulated shear capacity (based on laboratory test results)

Shear testing case	Scale, m (kN)	Shape, k	Mean, (kN)	COV (%)
0.46 m deep beams tested at 6 span to depth ratio	415	12	397	11

Table 6.9 Shear strength parameters based on the experimental data.

Shear testing case	Mean, (MPa)	COV, (%)
0.46 m deep beams tested at 6 span to depth ratio	5.01	11

From the shear strength values presented in Tables 5.18 and 6.9 a consistent reduction in the shear strength with the shear volume increment was observed. This is an indication of a significant size effect in shear beams.

A visual comparison of the 0.30 m and 0.46 m deep shear beams discussed above is given in Figure 6.7

Figure 6.7 Visual comparison of 0.30 m and 0.46 deep shear beams at 6 span to depth ratio

Shearing occurred within a couple of mille second's time and is difficult to observe in real time. Therefore, a high speed video camera was used to track and to confirm the shear failure. Images from this video taken in a mille-second interval are shown in Figure 6.8. Here the failure surface can be tracked by the dislocation of the vertical grids along the length of the beam.

Figure 6.8 Shear failure images from a high speed video

T= t + 0 milli-sec.

T= t + 1 milli-sec.

T= t + 2 milli-sec.

T= t + 3 milli-sec.

About twenty five percent of the beams broke in bending mode. In a couple of cases the failures were initiated by the tensile cracks and the ultimate failure occurred in shear. The load vs. stroke curve for a typical ultimate shear failure followed by an initial tensile crack is plotted in Figure 6.9. The sudden drop in load level after the initial failures was due to the changes in the net modulus of elasticity after the preceding break.

Figure 6.9 Load vs. Stroke curve for a 0.46 m deep glulam shear test

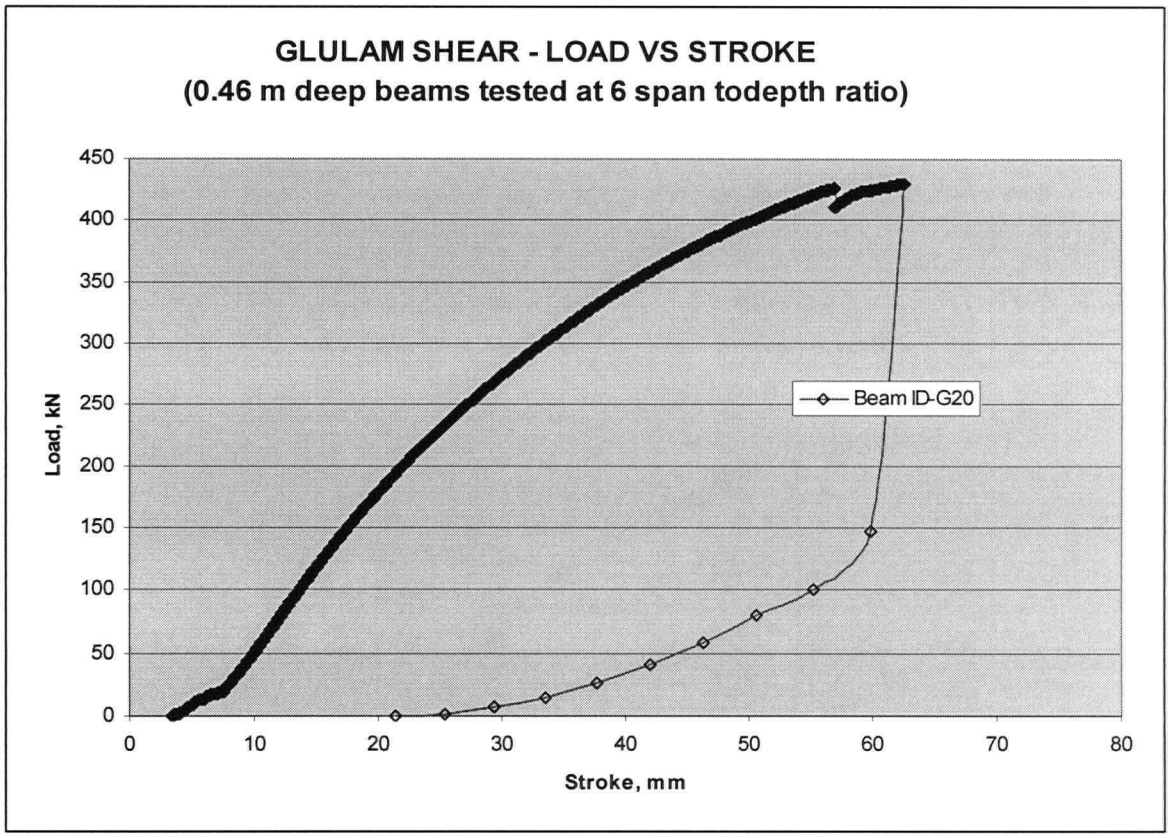

6.4 ULAG VERIFICATION

The verification tests demonstrate the ULAG's precision in predicting the flexural and shear strength capacities of the glue laminated timber beams. A comparison of the

bending test results and ULAG predictions for the specified strength and modulus of elasticity are given in Tables 6.10 and 6.11, respectively. A similar analysis for the shear strength is given in Table 6.12.

Table 6.10 Comparison between bending test results and ULAG prediction – specified strength

Beam case	Glulam specified strength		
	laboratory test results (MPa)	ULAG simulations (MPa)	Error %
0.61 m deep beam 18 span/depth ratio	32.2	32.7	1.6

Table 6.11 Comparison between bending test results and ULAG predicted MOE

Beam case	MOE		
	laboratory test results (MPa)	ULAG simulations (MPa)	Error %
0.61 m deep beams at 18 span/depth ratio	12,923	12,278	-5.0

Table 6.12 Comparison between shear test results and model prediction

Beam depth, m	Span to depth ratio	Simulated shear strength, MPa	Tested shear strength, MPa	Error, %
0.46	6	4.8	5.0	-2.9

From the results presented in Tables 5.10, 5.11, 5.20, 6.10, 6.11 and 6.12 a very accurate ULAG prediction with a maximum error of 1.6% observed for the glulam flexural strength and a maximum error of 5.4% observed for the glulam shear strength predictions. These errors are around -5% for the MOE assessments.

6.4.1 INFLUENCE OF FINGER JOINTS

The number of finger joints present in the tension side of the beam lay-up is expected to have significant impact on the overall capacity of the Glulam beam. Further during the laboratory tests and ULAG simulations a significant number of finger joint failures were observed. Therefore, a ULAG assessment was carried out to investigate the influence of finger joints on the overall flexural capacity of the glulam beam. The beam lay-up given in Table 6.2 was used with 18 span to depth ratio and third point loading setup. The summary of the assessments are given in Table 6.13.

Table 6.13 Comparison between the capacities of glulam beams constructed with different length of lamina stocks

Parameters		The ratio between 4.88 m and 2.44 m long boards in the samples corresponding to each of the lamina grade		
		75:25 (Case 1)	50:50 (Case 2)	25:75 (Case 3)
Beam Depth, h, cm		60.6	60.6	60.6
L/h ratio		18	18	18
Number of finger joints per 100 lamina layers*		61	92	122
Ultimate Failure Load, kN	Mean	182.2	179.8	176.6
	SD	23.5	22.6	21.2
MOR, MPa	Mean	42.2	41.8	41.8
	SD	5.4	5.8	5.8
Rs , MPa		33.3	32.2	32.2

**Number of finger joints observed at the middle 3.5 m segment of the beam layer*

For the cases investigated it was observed that the changes in the number finger joints, for example a variation of the presence (middle 3.5 m length of the beam was considered for this observation) of number of finger joints from sixty finger joints per hundred lamina layers (case 1) to hundred and twenty finger joints per hundred boards

(case 3), has a 3% impact on the overall flexural capacity of the 0.61 m deep glulam beam simulated with 11.0 m test span.

6.5 SIZE EFFECTS IN BENDING

ULAG beam simulations account for the presence of two major defects within a glulam beam; the effects of knot distributions (defects) and the finger joints. Therefore, ULAG can be used directly to study the glulam-size/volume factors.

A glulam size effect study was carried out for Douglas fir glulam beams. Three beams with depths of 0.30 m, 0.61 m and 0.91 m were used for the assessments. The 0.30 m deep beam lay-up A8U given in Table 5.4 with a span to depth ratio of 12 was used as the primary lay-up. In order to avoid any influence of the beam configuration, the ratio of the various grades of lamina in the 0.61 m and 0.91 m was kept as similar to the 0.30 m deep beam. The details of the beam lay-ups considered for the assessments are given in Table 6.14.

Table 6.14 Beam lay-ups used for the volume effect analysis

Beam case	Lamina number (from the bottom of the beam)																							
	24	23	22	21	20	19	18	17	16	15	14	13	12	11	10	9	8	7	6	5	4	3	2	1
1																	Cc	C	D	D	D	D	C	T1
2									Cc	Cc	C	C	D	D	D	D	D	D	D	D	C	C	T1	T1
3	Cc	Cc	Cc	C	C	C	D	D	D	D	D	D	D	D	D	D	D	D	C	C	C	T1	T1	T1

The beams were evaluated using ULAG under third point loading in a simulation study with 1000 replications. The summary of the size effect analysis is given in Table 6.15.

Table 6.15 Summary of the size effect analysis

Depth, m	Test span, m	Beam volume, V, m^3	Failure load		MOR (mean), MPa
			Mean, kN	COV, %	
0.30	3.66	0.14	164	17	48.1
0.61	7.32	0.58	314	12	45.9
0.91	10.97	1.3	441	12	43.0

The relationship between the size factor k, MOR, and beam volume V for beams having same span to depth ratio can be given by the following equation.

$$\log(MOR) = -\frac{1}{k}\log(V) + C \text{, C is a constant} \qquad (6.1)$$

A plot of log (V) vs. log(MOR) along with a linear trend line is shown in Figure 6.10.

Figure 6.10 Variation of log(MOR) with log(V) for the glulam beam cases considered in the volume effect analysis

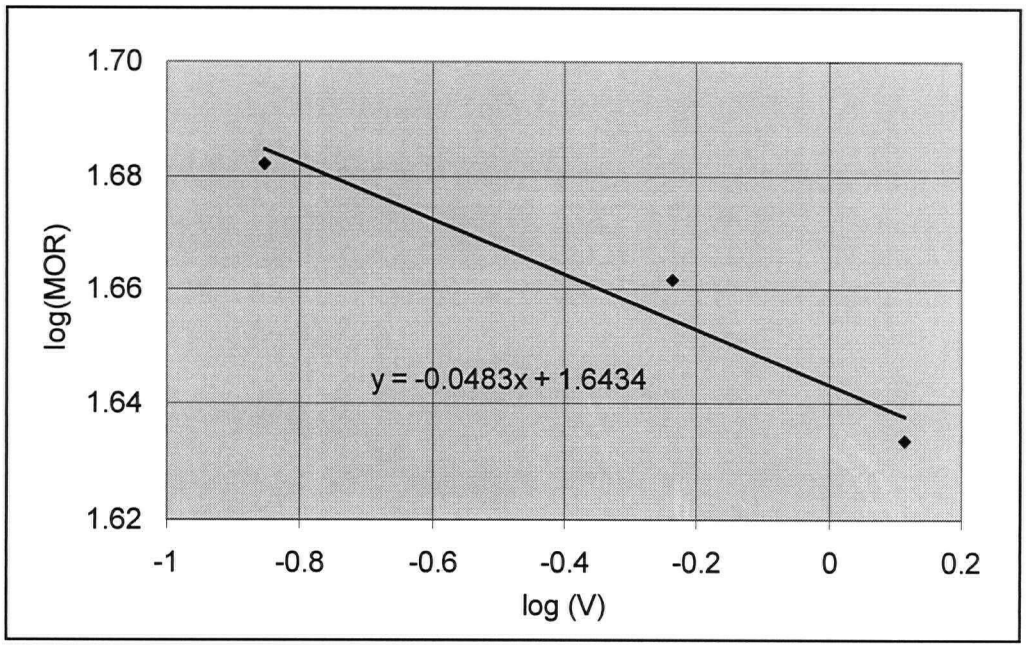

From the gradient of the line, the size-effect factor k = 21. However, the size factor used in the Canadian Standard CAN/CSA O86.1-M89 is 5.4 with the beam width and length as parameters; i.e., beam depth is not explicitly considered. Subsequently the variations of MOR values with volume were investigated with different size-effect factors (Figure 6.11). The k value provided in the standard seems too conservative for beams smaller than the standard beam size (0.13 m x 0.61 m x 9.1 m) but non-conservative with the beam larger than the standard beam size. More work is needed to experimentally confirm the k factor using large beams.

Figure 6.11 Comparison of the variation of log(MOR) with log(V) with different size effect factors (V in units of m^3 and MOR in units of MPa)

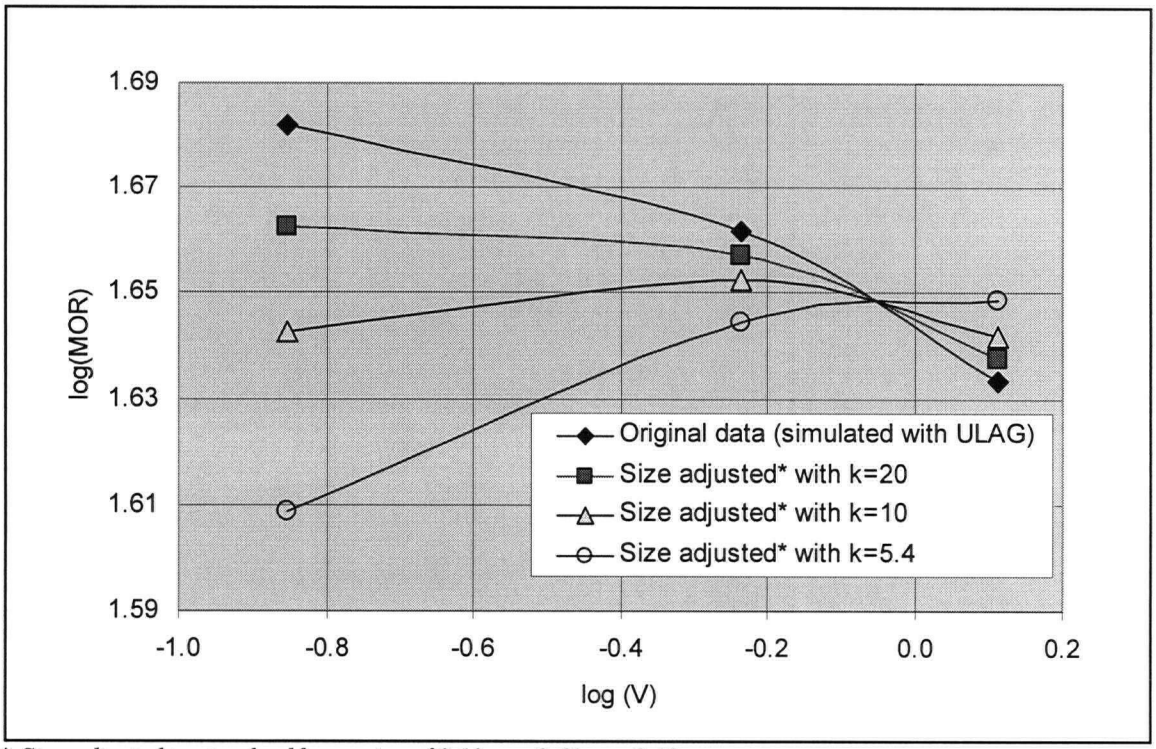

* *Size adjusted to standard beam size of 0.13 m x 0.61 m x 9.10 m.*

6.6 FLEXURAL STRENGTH AND STIFFNESS COMPATIBILITIES

When developing new lay-up for glulam beams, it is common to place the grades with high flexural strength and MOE at the extreme tension zone of the beam to increase the beam's flexural capacity. During ULAG simulations it was observed that the combining effect of the laminae strength and stiffness plays a significant role in controlling the ultimate beam capacity.

The detail of this analysis is given below.

Two beam lay-ups C1 and C2 shown in Table 6.16 were considered for the analysis. The difference between these lay-ups is that the extreme tension lamina grade B in C1 is replaced by a better T1 grade in C2. The key strength parameters of the grades T1 and B are given in Table 6.17. At this point C1 is expected to be weaker than C2. Subsequently ULAG beam simulations were performed on these lay-ups and the results are tabulated in Table 6.18 These lay-ups had average MOE values of 11,900 MPa and 12,100 MPa respectively.

Table 6.16 Glulam beam lay-ups used for the special investigation

	Lamina number (from the bottom of the beam)															
Beam lay-up ID	16	15	14	13	12	11	10	9	8	7	6	5	4	3	2	1
C1	Cc	Cc	C	C	D	D	D	D	D	D	D	D	C	C	B	B
C2	Cc	Cc	C	C	D	D	D	D	D	D	D	D	C	C	B	T1

Table 6.17 Key strength parameters of the grades T1 and B

Lamina grade	Tensile strength, MPa (2.44 m gauge length)	Tensile strength of the finger joints, MPa	Average, E, MPa
T1	50	42	15,200
B	35	40	13,700

Table 6.18 Results of the special investigation

	Progressive failure (ultimate load), kN		First failure loads, kN	
Beam lay-up ID	C1	C2	C1	C2
Mean	187.1	181.3	142.1	148.9
SD	20	24	24	24

ULAG predicts higher mean ultimate failure loads for C1 (187 kN) than C2 (181 kN). The first failure data shows C2 is stronger than C1.

In C2 due to the higher stiffness of the T1 grade compared to the B grade lamina, higher stress are expected to be developed in the T1 layer in C2 compared to the B layer in the C1. Even though the T1 grade laminae are stronger than the B grade laminae, the finger joint strengths for these laminae are similar. Therefore in the C2 beam ended up to be weaker than the C1 beam. This finding is not unique and was previously observed in older studies. Therefore, further investigation on this is recommended.

6.7 RELIABILITY ANALYSIS

The ULAG simulations described previously focused on analyzing the simple load carrying capacity of the glulam beams. One important concern is the reliability or the chances of failure of the beam under a general loading condition. In this way a reliability analysis was carried out to study the general performance of the beams/beam lay-ups. The assessment was carried out for the 0.30 m and 0.61 m deep glulam beams used for the calibration and verification tests. The analysis was preformed with the common reliability parameters acceptable in general situations as given below:

The performance function can be written as

$$G = R - (E(D) + E(Q)) \tag{6.2}$$

E(D) and *E(Q)* are the design dead and live loads , respectively.

After substituting the appropriate parameters for E(D) and E(Q) equation 6.2 can be re-written as fallows.

$$G = R - \frac{3Q_n L^2}{4bh^2}(d\gamma + q) \tag{6.3}$$

where, L - loading span of the beam, b - width of the beam, h – height of the beam, R - bending strength; MOR (assuming a normal distribution, obtained from ULAG simulation), Q_n - nominal live load and d and q are the dead and live loads normalized with respect to their corresponding design values.

$$\gamma = \frac{D_n}{Q_n} = 0.25$$

$$d = \frac{D}{D_n} = 1 + V_D R_n ; \quad V_D = 0.10, \quad R_n = \text{ standard normal random variable}$$

here R, R_n, Q_n and q are random variables.

Following load data and other conditions were used based on the provisions given by Foschi et al. (1989)

(i) Target reliability $\beta = 3.0$

(ii) Occupancy loads (Extreme type I distribution), for offices corresponds to maxima over 30 years return period.

$q_{(mean)} = 0.925$ and $q_{(COV)} = 0.236$

(iii) Vancouver snow load with 30 years of return period.

$Q_{n(mean)} = 0.0014$ MPa and $Q_{n(COV)} = 0.287$.

Second order reliability analyses were carried out using the computer program RELAN (Foschi and Folz 1992). A trial and error beam spacing varying from 3 m to 5 m was used to find the optimum beam spacing corresponds to the target reliability. The summary of the reliability analysis results is given in Table 6.19.

Table 6.19 Summary of the reliability analysis

Beam lay-up	Parameters	Beam spacing, m		
		3.0	4.0	5.0
A8U	β	4.3	3.3	2.6
	Probability of failure	9.0E-04	4.0E-02	4.6E-01
A5U	β	4.8	3.9	3.1
	Probability of failure	9.3E-05	5.5E-03	8.9E-02

As mentioned earlier the target reliability index (β) of the analysis is 3.0. Therefore, 4.0 m spacing is recommended for 0.30 m deep beams with 21 span to depth ratio and 5.0 m spacing is recommended for 0.61 m deep beams with 18 span to depth ratio.

Chapter 7

Concluding Remarks

7.1 SUMMARY

Canadian glulam industry has a resource optimization issue related to the supply of the high grade laminae material required for the glulam manufacturing. From the manufacturers' point of view there is a need for some modification in the current grade specifications in order to fairly match the supply and demand of the material resources, especially for the high grade material placed at the extreme tension zone. Here the main concern is to develop a new laminae grade set focusing on increasing the efficient use of lamina on construction of 24f glulam beams. In this way specifications for a set of five Douglas fir lamina grades T1, Cc, B, C and D were developed and the grade outturn was established based on subsequent grading and analysis.

Initially the new lamina grade boards are subjected to knot survey in order to qualify the new lamina grades according to ASTM D3737. The data were analyzed using the computer program GAP and a satisfactory performance was reported. Samples from each of the new laminae set were E rated. Furthermore samples of laminae and finger joints of the tension lamina grades T1, B, C and D were tested in tension to establish the strength of the laminae and finger joints corresponding to the new grades.

Modifications were done in the ULAG program to make it compatible to the Windows XP versions. Then a procedure to account for the laminating factor and subroutines required to perform the shear capacity assessment were developed and incorporated with ULAG. The shear assessments were performed based on the weakest link stress volume theory. The shear stress outputs from the finite element analysis was

integrated and compared to the strength of a small clear specimen at a common probability of interest to predict the shear capacity of the full scale glulam beam.

Then a series of ULAG analysis were performed and a 0.30 m deep 24f glulam beam was successfully simulated using the refined ULAG program. A set of twenty four 0.30 m deep glulam beams were tested with 21 span to depth ratio to as part of ULAG calibration process. Very small errors between the ULAG predicted flexural capacity and test results were observed. Two sets of 0.30 m deep glulam beams were tested at short span to determine the shear capacity. This information was used to fine tune the clear wood strength parameters used in the shear capacity assessment model.

Subsequently two sets of forty eight 0.61 m and 0.45 m deep glulam beams were tested in bending and shear, respectively to verify model predictions. The bending strength and MOE of the 24f glulam verification tests agreed very precisely with ULAG predictions. As intended a sufficient number of pure shear failures were obtained to predict the shear strength capacity. The MLE method was used to predict the pure shear capacity of the beams considered. Subsequent analyses confirmed the significant of size factor in shear.

7.2 CONCLUSIONS

The current study provides many results/research findings in relation to the modeling of glulam beams. Some of the key outcomes are given below :

1. A new grade set consisting five new glulam lamina grades T1, Cc, B, C and D was developed and validated for the manufacturing of the 24f glulam beams.

2. The accuracy of ULAG in simulating the flexural strength of glulam was demonstrated.
3. The new ULAG model also predicts the shear capacities of glulam with sufficient confidence.
4. A significant size effect in shear was verified.

ULAG program predicted some initial failures at the inner D grade layers of the beam which are generally not expected to break. High speed videos taken during the beam testing also confirm some initial inner failures to some extent. This finding shows the efficiency of ULAG in assessing the performance of the glulam-lay-up combinations.

As predicted by ULAG, a very low strength glulam beam in bending was found at the lower tail of the distribution during testing. Subsequent investigation identified it to be caused by a knot failure at the 2nd tension (inner) layer.

The procedures established from this study demonstrate a new method for glulam beam lay-up design and assessment by using ULAG to predict the flexural capacity of Glulam beams as well as using the tensile strength and the corresponding MOE values of the lamina and the tensile strength of the finger joints as input.

Other significant outcomes of the study are the details of the material properties obtained for the Douglas fir laminating grade boards.

1. Knot survey/knot mapping information
2. Tensile strength distribution
3. Finger joint strength distribution
4. MOE data for laminae

7.3 JUSTIFICATIONS

The full scale shear strength tests of this kind are unique. The beam lay-up for the shear tests was made based on the ULAG predictions. During these assessments the lay-up was made targeting a significant number of shear failures as resulted. Since the data contain both bending and shear failure modes, the shear beam test results were subsequently analyzed using MLE procedures to obtain un-censored data.

The model assessments and the laboratory testing were focused on flexural strength and shear strength. During the modeling and testing it was assumed that the glue bond in between the laminae is very strong. There were no significant delamination failures observed during the full scale beam testing.

There were couples of minor compression deformation observed near the top layers. This again was treated as insignificant, with the justification that there was no noticeable beam failures observed related to these deformations.

7.4 SUGGESTIONS FOR FUTURE RESEARCH

Even though the ULAG predictions made a significant revolution in the development of glulam lay-up, the complicated internal stresses near the supports and loading points need careful consideration. Investigations on these issues may further enhance the model predictions.

Current analysis produces a strength distribution for the 38 mm x 140 mm Douglas fir laminating grades. It is recommended to expand this data- base incorporating the strength profile of other key species such as Hem fir, etc. and different member widths.

The compatibility issue related to the flexural strength and modulus of elasticity presented in section 6.6 is an issue of interest, especially when designing new beam construction. It is recommended to verify this by means of further full scale laboratory testing.

Calibration/Verification of ULAG for the glulam tension and compression loading cases will be another constructive step in upgrading ULAG for more efficient glulam design and analysis.

The type of the glulam supports and connections widely differ depending on the structural applications considered. These factors may develop different types of stress interactions across the beam. It is recommended to investigate the influence of the supports and connectors on the overall capacity of the glulam beam.

Bibliography

AITC. 2004. Standard specifications for structural glued laminated timber of softwood species. AITC 117-2004, American Institute of Timber Construction, Centennial.

APAEWS. 2003. Glulam Product Guide. Form No. EWZ X440B, Engineered Wood Systems-APAEWS, Tacoma, Washington.

ASTM. 2006. Test methods for mechanical properties of lumber and wood-based structural material. Standard ASTM D 4761, American Society for Testing Materials, West Conshohocken, Pa.

ASTM. 2006. Standard methods of static tests of timber in structural sizes. Standard ASTM D 198, American Society for Testing Materials, West Conshohocken, Pa.

ASTM. 2006. Practice for Establishing allowable properties for structural glued laminated timber (Glulam). Standard ASTM D 3737, American Society for Testing Materials, West Conshohocken, Pa.

Bathe, K.J. 1982. Finite element procedures in engineering analysis, Prentice-Hall Inc., Englewood Cliffs, New Jersey. 735 p.

Bodig, J. and Jayne, B.A 1982. Mechanics of wood and wood composites, Van Nostrand Reinhold, Co., New York. 712 p.

Buchanan, A.H. 1984. Strength model and design methods for bending and axial load interaction in timber members. Ph.D. Thesis, The University of British Columbia, Vancouver, Canada. 298 p.

Cramer, H. and Leadbetter. M.R. 1967. Stationary and related stochastic process; sample function properties and their applications. John Wiley & Sons, New York. 348 p.

CSA. 1989. Engineering design in wood (limit states design). Standard CAN/CSA O86.1-M89, Canadian Standards Association, Rexdale, Ont.

CSA. 1989. Qualification code for manufacturers of structural glued-laminated timber. Standard CAN/CSA-O177-M89, Canadian Standards Association, Rexdale, Ont.

CSA. 1989. Structural glued-laminated timber. Standard CAN/CSA-O122-M89, Canadian Standards Association, Rexdale, Ont.

Falk, R. and Colling, F. 1994 Glued –laminated timber: laminating effects. Proceeding of the Pacific Timber Engineering Conference, Gold Coast Australia, July. 11-15.

Falk, R. and Colling, F. 1994 Laminating effects in glued-laminated timber beams. Journal of Structural Engineering, ASCE, 121(12): 1857-1863.

Folz, B. and Foschi, R.O. 1992. Stochastic finite element analysis of laminated beams. Annual Conference of the Canadian Society for Civil Engineering, Quebec, May 27-29.

Folz, B. and Foschi, R.O. 1993. ULAG: Ultimate load analysis of glulam-user's manual. Version 1.0, Department of Civil Engineering, The University of British Columbia, Vancouver, Canada. 23p.

Folz, B. and Foschi, R.O. 1994. Stochastic finite element analysis of progressive failure in a laminated wood beam, in: Schueller, Shinozuka, Yao (Eds.), International Conference on Structural Safety and Reliability, ICOSSAR 93, Balkema, Rotterdam, 1994. 585-592.

Folz, B.R. 1997. Stochastic finite element analysis of the load-carrying capacity of laminated wood Beam-Columns. Ph.D. Thesis, The University of British Columbia, Vancouver, Canada. 163 p.

Foschi, R. O. and Barrett, J.D. 1976. Longitudinal Shear in Wood Beams: a design method. Canadian Journal of Civil Engineering, NRC Canada, 3: 199-208.

Foschi, R. O. and Barrett, J.D. 1977. Longitudinal Shear in Wood Beams: a design method. Canadian Journal of Civil Engineering, NRC Canada, 4: 363-369.

Foschi, R. O. and Barrett, J.D. 1980. Glued-Laminated Beam Strength: A Model. Journal of the Structural Division, ASCE, 106(ST8): 1735-1754.

Foschi, R. O., Folz, B. and Yoa, F. Z. 1993. RELAN: RELiability ANalysis -user's manual, Version 2.24. Department of Civil Engineering, The University of British Columbia, Vancouver, Canada.

Foschi, R. O., Folz, B. and Yao, F.Z. 1989. Reliability-based design of wood structures. Structural Research Series, Report No. 34, Department of Civil Engineering, The University of British Columbia, Vancouver, Canada.

Hernandez, R., Bender, D.A., Richbur, B.A. and Kline, K.S. 1992. Probabilistic modeling of glued-laminated timber beams. Wood and Fiber Science, The Society of Wood Science and Technology, 24(3): 294-306.

Heylinger, P.R. and Reddy, J.N. 1988. A higher order beam finite element for bending and vibration problems. Journal of Sound and Vibration, 126(2): 309-326.

Klapp, H. and Brüninghoff, H. 2005. Shear Strength of Glued Laminated Timber. Proceedings of the International Council for Research and Innovation in building and Construction, Working Commission W18- Timber Structures. 38th meeting, Karlsruhe, Germany, August 2005.

Koka, E.N. 1987. Laterally loaded wood compression members: Finite element and reliability analysis. M.A.Sc. Thesis, The University of British Columbia, Vancouver, Canada. 120 p.

Lam, F. 2000. Length effect on the tensile strength of truss chord members. Can. J. Civ. Eng. NRC Canada, 27: 481-489.

Lam, F., Yee, H. and Barrett, J.D. 1997. Shear strength of canadian softwood structural

lumber. Can. J. Civ. Eng. NRC Canada, 24: 419-430.

Lee, J.J., Kim, K.M. and Oh, J.K. 2005. Prediction of bending properties for structural glulam using optimized distributions of knot characteristics and laminar MOE. Journal of Wood Science, The Japan Wood Research Society, 51: 640-647

Marx, C.M. and Evans, J.W. 1986. Tensile strength of AITC 302-24 grade tension laminations. Forest Prod. J. 36(1): 13-19

Marx, C.M. and Evans, J.W. 1988. Tensile strength of laminating grades of lumber. Forest Prod. J. 38(7/8): 6-14

Melchers, R.E. 1987. Structural reliability analysis and prediction. Ellis Horwood Limited, Chichester. 437 p.

Moody, R. C. and Hernandez, R. 1997. Glued-laminated timber. In: Smulski, Stephen, Ed., Engineered wood products-A guide for specifiers, designers and users. Madison, WI. Chapter 1. 1-139.

Moody, R., Falk, R. and Williamson, T. 1990. Strength of glulam beams – volume effects. 1990 International Timber Engineering Conference, Tokyo, Japan. 176-182.

Moody, R.C. and Falk, R.H. 1989. Development of design stresses for glulam timber in the United States. Proceeding or the 2nd Pacific Timber Engineering Conference, Auckland New Zealand, Aug. 28-31, vol. 2. 309-313

Rammer, D.R. 1997. Shear strength of solid-sawn Douglas-fir beams. Journal of Materials in Civil Engineering, ASCE, 9(3):130-138.

Rammer, D.R., Soltis, L.A. and Lebow, P.K. 1996. Experimental shear strength of unchecked solid-sawn Douglas-fir. Research Paper FPL-RP-553, Madison, WI: US. Department of Agriculture, Forest Service, Forest Products Laboratory. 33p.

Steiger, R. and Köhler, J. 2005. Analysis of censored data-examples in timber engineering research. Proceedings of the International Council for Research and Innovation in building and Construction, Working Commission W18- Timber Structures. 38th meeting, Karlsruhe, Germany, August 2005.

Timusk, P.C. 1997. Experimental evaluation of the ULAG glulam beam simulation program. M.Sc. Thesis, The University of British Columbia, Vancouver, Canada. 80 p.

Yeh, B. and Williamson, T.G. 2001. Evaluation of glulam shear strength using a full-size four-point test method. Proceedings of the International Council for Research and Innovation in building and Construction, Working Commission W18- Timber Structures. 34th meeting, Venice, Italy, August 2001.